

Abstract

We examine how Sudden Commencements (SCs) and Storm Sudden Commencements (SSCs) influence the occurrence of high rates of change of the magnetic field (R) as a function of geomagnetic latitude. These rapid, high amplitude variations in the ground-level geomagnetic field pose a significant risk to ground infrastructure, such as power networks, as the drivers of geomagnetically induced currents.

We find that rates of change of $\sim 30 \text{ nT min}^{-1}$ at near-equatorial stations are up to 700 times more likely in an SC than in any random interval. This factor decreases with geomagnetic latitude such that rates of change around 30 nT min^{-1} are only up to 10 times more likely by 65° .

At equatorial latitudes we find that 25% of all R in excess of 50 nT min^{-1} occurs during SCs. This percentage also decreases with geomagnetic latitude, reaching $\leq 1\%$ by 55° . However, the time period from the SC to three days afterwards accounts for $\geq 90\%$ of geomagnetic field fluctuations over 50 nT min^{-1} , up to $\sim 60^\circ$ latitude. Above 60° , other phenomena such as isolated substorms account for the majority of large R . Furthermore, the elevated rates of change observed during and after SCs are solely due to those classified as SSCs.

These results show that SSCs are the predominant risk events for large R at mid and low latitudes, but that the risk from the SC itself decreases with latitude.

Plain Language Summary

Rapid changes in the Earth's magnetic field can create the conditions for anomalous and potentially dangerous currents in spatially large networks such as power lines and pipelines. One phenomenon that can cause such rapid changes in the magnetic field are Sudden Commencements (SCs), driven by interplanetary shocks impacting the Earth's magnetosphere. In this work, we assess the risk due of SCs, finding that they contribute a significant fraction of large rates of change of the ground field at mid and low latitudes. SCs may also be followed by geomagnetic storms, and if we consider both the short SC intervals as well as a three day period that follows we can account for the vast majority of large rates of change of the geomagnetic field, at mid and low latitudes. This work should help guide hazard estimates for energy providers, for example the time period after an SC in which they could expect large and potentially dangerous currents.

1 Introduction

One of the main pathways through which Space Weather can impact society is through damage to ground-based infrastructure caused by the generation of Geomagnetically Induced Currents (GICs). GICs originate from the induced Ground Electric Field (GEF), which itself is driven by high amplitude magnetic field fluctuations and geological conductivity gradients. GICs can be generated in any long grounded conductor, including power grids, pipelines or rail networks (Boteler et al., 1998). Modern society is fundamentally dependent upon the reliable delivery of power, and Space Weather is therefore a critical risk factor for such operations (e.g. Eastwood et al., 2018; Committee on the Peaceful Uses of Outer Space (COPUOS), 2017). The impact of widespread power network failure has been estimated at billions of US dollars a day (Oughton et al., 2017, 2019).

Direct measurements of GICs in infrastructure are sparse, either due to their commercial sensitivity or expense in performing the observations. The South Island of New Zealand is a notable exception (e.g. Marshall et al., 2012; Mac Manus et al., 2017; Rodger et al., 2017). Indirect observations of GICs in power lines are also possible, using techniques such as the differential magnetometer method (e.g. Campbell, 1980; Viljanen & Pirjola, 1994; Hübner et al., 2020), however these measurements are also sparse since ad-

ditional equipment needs to be deployed and data analyzed. Therefore, for geographically widespread and long time interval studies a substitute measurement is required.

The magnitude of GICs in a given power network is dependent upon three main factors: the rate of change of the surface magnetic field, the orientation and properties of the power network and the local geology (i.e. the subsurface conductivity) (Thomson et al., 2005; Viljanen et al., 1999, 2013; Beggan, 2015; Bedrosian & Love, 2015; Divett et al., 2018). The time scales of magnetic field variability have also been shown to be significant, with certain frequencies of magnetic field variability showing the best match with observed GICs (Oyedokun et al., 2020; Clilverd et al., 2020). However, in general, larger rates of change of the geomagnetic field will drive larger GICs (Viljanen et al., 2001). Indeed recent concurrent measurements from New Zealand have confirmed that the rate of change of the horizontal magnetic field is very well correlated with the observed GIC magnitude (Mac Manus et al., 2017; Rodger et al., 2017). Since the ground-level magnetic field has been consistently measured around the globe for many decades, this provides an appropriate proxy dataset to statistically examine the potential likelihood of large GICs at different latitudes.

There are a plethora of phenomena, ultimately driven by the interaction between the solar wind and the Earth's magnetosphere, that can result in elevated rates of change of the ground magnetic field. On the largest spatial and temporal scales, geomagnetic storms are driven by significant periods of enhanced coupling between the solar wind and magnetosphere, typically by Coronal Mass Ejections (CME) and their surrounding medium (Borovsky & Denton, 2006; Richardson & Cane, 2012; Kilpua et al., 2019). For many years geomagnetic storms and related smaller scale storm associated dynamical processes have been linked to variations in the geomagnetic field, and further to induced currents (Kappenman & Albertson, 1990; Kappenman, 1996; Pulkkinen et al., 2005; Ngwira, Pulkkinen, Leila Mays, et al., 2013; A. Dimmock et al., 2019). On a shorter time scale of hours, geomagnetic substorms, which manifest as cycles of energy storage and release in the magnetosphere (e.g. Akasofu, 1964; McPherron et al., 1973; Tanskanen et al., 2002), are also associated with the generation of dynamic ionospheric currents. Substorms are sporadic and intermittent, but tend to recur on time scales of approximately 2 - 4 hours during periods of strong solar wind driving (Huang et al., 2004; Freeman & Morley, 2004; Lee et al., 2006; S. Morley et al., 2009; Forsyth et al., 2015). While ionospheric currents vary with local season, the average additional dynamic currents resulting from substorms are similar throughout the year (Forsyth et al., 2018). The strong and dynamic ionospheric substorm currents often correspond to large changes in the geomagnetic field (Viljanen et al., 2001; Turnbull et al., 2009; Freeman et al., 2019; Engebretson et al., 2021), and GICs (Viljanen et al., 2006). Studies have shown that high-latitude surface magnetic field perturbations, and the field-aligned currents that drive them, react to the solar wind on different characteristic time scales: ranging between 10 and 150 minutes depending on location (e.g. Coxon et al., 2019; Shore et al., 2019).

In contrast to the energy storage and release processes within a substorm, some intervals of large ground magnetic variability can be driven by much more immediate changes in the impinging solar wind, for example Sudden Commencements (SCs). SCs are rapid increases in the northward component of the ground magnetic field (Chree, 1925; Araki, 1977; Araki et al., 1997), signaling the response of the magnetosphere to the impact of a solar wind pressure pulse or shock (Takeuchi et al., 2002; Lühr et al., 2009; Fiori et al., 2014; D. Oliveira & Samsonov, 2018). Such changes in the geomagnetic field have also been commonly noted to generate large GICs (e.g. Kappenman, 2003; Beland & Small, 2004; Marshall et al., 2012; Carter et al., 2015; Zhang et al., 2015; Rodger et al., 2017; D. M. Oliveira et al., 2018). These interplanetary shocks may be driven by structures such as CMEs, and so while the initial shock may drive or instigate immediate magnetospheric activity, it may also herald the start of a longer interval of enhanced coupling between the solar wind and magnetosphere - the geomagnetic storm, that includes a wide

118 range of magnetospheric phenomena such as geomagnetic substorms (Kokubun et al.,
 119 1977; Akasofu & Chao, 1980; Gonzalez et al., 1994; Zhou & Tsurutani, 2001; Yue et al.,
 120 2010). An SC that is followed by a geomagnetic storm is referred to as a Storm Sudden
 121 Commencement (SSC).

122 Rogers et al. (2020) recently used extreme value theory to show that the distribu-
 123 tion of return rates of extreme surface magnetic field variability vary significantly with
 124 local time and latitude, with evidence for distinct driving phenomena being discernible.
 125 For example, at low latitudes a class of extreme rates of change of the field were mostly
 126 northward directed, and therefore likely attributable to SCs. Meanwhile, several authors
 127 have shown that the magnitude of extreme geomagnetic fluctuations (at the 100 - 200
 128 year return level) maximise between approximately 50 and 60° geomagnetic latitude, cor-
 129 responding to the maximum equatorward extent of the auroral electrojets (Thomson et
 130 al., 2011; Ngwira, Pulkkinen, Wilder, & Crowley, 2013; Rogers et al., 2020). While these
 131 large scale patterns are observed, it should be noted that local effects, either from sharp
 132 spatial conductivity changes or small-scale ionospheric currents, may also have a signif-
 133 icant effect on the precise measured magnetic field variability (e.g. Ngwira et al., 2015;
 134 A. P. Dimmock et al., 2020). It is therefore of crucial importance to consider the vari-
 135 ability of the magnetic field as a function of both local time and latitude.

136 Recently, Freeman et al. (2019) and Smith et al. (2019) assessed the relative con-
 137 tribution of substorms and SCs (respectively) to extreme ground magnetic field variabil-
 138 ity at the mid-latitude UK magnetometer stations. Freeman et al. (2019) found that 54–
 139 56% of extreme ($\geq 99.97th$ percentile) ground fluctuations in the UK were associated
 140 with substorm expansion and recovery phases, explaining a large portion of such vari-
 141 ability, but leaving a relatively large fraction unattributed. Meanwhile, Smith et al. (2019)
 142 showed that only a small fraction ($\leq 8\%$) of extreme rates of change of the geomagnetic
 143 field were associated directly with SCs, but that 90% of all extreme fluctuations were
 144 observed in the 3 days following SSCs, thereby including each SSC’s storm and compo-
 145 nent substorms that are causally related to the same solar wind structures. The scope
 146 of the study by Smith et al. (2019) was extremely limited in latitude, only considering
 147 three mid-latitude, UK based stations. In this work, we expand this scope to consider
 148 the relative impact of SCs on ground magnetic field variability at a large number of mag-
 149 netometer stations. In particular we assess how the impact of SCs varies with geomag-
 150 netic latitude. The study is structured as follows. First, in Section 2 we outline the data
 151 and definitions used by the study. In Section 3 we discuss the results of the study, while
 152 in Section 4 we discuss our results in terms of the latitudinal dependence observed, the
 153 type of magnetospheric response and consequences for forecasting GICs. Section 5 then
 154 summarizes the study.

155 2 Data

156 In this study we utilize one minute resolution data from a collection of INTERMAG-
 157 NET observatories. We have selected magnetometer stations as close in longitude to the
 158 three UK based stations in the original study of Smith et al. (2019) as possible, while
 159 attempting to maximize our latitudinal coverage. In this way we attempt to minimize
 160 any local time effects that could be present (c.f. Rogers et al., 2020). We further require
 161 that data from the observatory is available for the full interval between 1996 and 2016
 162 (inclusive), which forms the basis of our statistical study. As SCs are a stochastic phe-
 163 nomenon, it is vital to ensure the data set and events are identical between stations. A
 164 map of the 12 stations fulfilling these criteria is shown in Figure 1, Table 1 provides fur-
 165 ther details. The geomagnetic latitudes were calculated using the International Geomag-
 166 netic Reference Field (IGRF) 2010 model. While we have attempted to cover as broad
 167 a latitudinal range as possible, it can be seen that the region between 44 and 65° geo-
 168 magnetic latitude is fairly densely represented, while there is a gap between 7 and 44°.

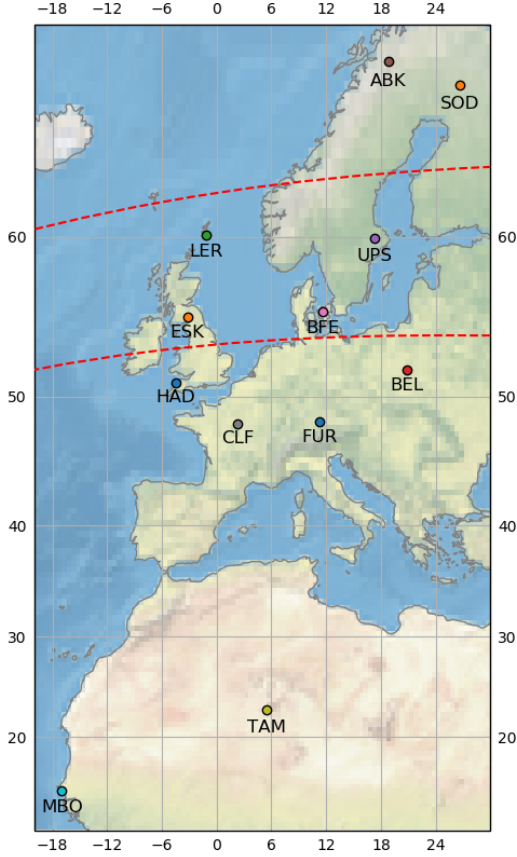


Figure 1. A geographical map of the 12 INTERMAGNET observatories included in this statistical study. The geomagnetic latitudes of 50° and 60° north are indicated with dashed red lines for reference. These geomagnetic latitudes have been calculated using a quasi-dipole model.

169 Nonetheless, this selection of stations provides us with adequate latitudinal sampling (as
 170 will be shown) and the long interval of data necessary for this study.

171 **2.1 Rate of Change**

172 We define the horizontal geomagnetic field as $\mathbf{H} = (X, Y)$, where X and Y are
 173 the northward and eastwards components respectively. We then define the one-minute
 174 rate of change of the horizontal geomagnetic field (R) as:

$$R = \frac{\delta \mathbf{H}}{\delta t} = \frac{\sqrt{[X(t + \delta t) - X(t)]^2 + [Y(t + \delta t) - Y(t)]^2}}{\delta t} \quad (1)$$

175 in order to capture directional changes as well as changes in magnitude, following
 176 the definition used by several studies in the literature (e.g. Viljanen et al., 2001; Free-
 177 man et al., 2019; Smith et al., 2019). This definition is also suitable for studies consid-
 178 ering GICs, for which field rotations may be significant (e.g. Beggan, 2015).

Table 1. INTERMAGNET observatories included in this study

Station Code	Station Name	Geomagnetic Latitude	Geomagnetic Longitude
ABK	Abisko	65.18	101.82
SOD	Sodankyla	63.81	107.29
LER	Lerwick	57.85	81.15
UPS ^a	Uppsala ^a	56.34	95.90
ESK	Eskdalemuir	52.86	77.39
BFE	Brorfelde	52.14	89.54
HAD	Hartland	48.12	74.79
BEL	Belsk	47.84	96.09
CLF	Chambon La Foret	44.12	79.35
FUR	Furstenfeldbruk	44.01	86.91
TAM	Tamanrasset	6.81	78.31
MBO	Mbour	0.11	57.85

^aData taken from the nearby LOV station prior to 2003.

179

2.2 Sudden Commencements

180

181

182

183

184

185

186

187

188

189

190

191

We utilize an independent catalog of Sudden Commencements (SCs), maintained by the International Service on Rapid Magnetic Variations (part of the International Service of Geomagnetic Indices), based at Ebre Observatory. These SC intervals have been identified based on inspection of the data from five low-latitude observatories (Curto et al., 2007), spaced around the globe in longitude as close to the magnetic equator as possible. The yearly catalogs can be found at <http://www.obsebre.es/en/rapid/>. We use the catalogs for the years 1996 - 2016 (inclusive). During this interval a total of 380 SCs were recorded which, given each SC is approximately 5 minutes in duration, cumulatively corresponds to approximately 1900 minutes of data. While the start and end of the SC magnetic signatures were determined manually, the average ~ 5 minute interval corresponds closely with the response time of the magnetopause to a solar wind shock (Freeman et al., 1995; Freeman & Farrugia, 1998).

192

193

194

195

196

197

198

199

200

201

202

203

204

SCs may be classified retrospectively based on whether a geomagnetic storm is observed in the hours following the SC. If a storm is observed then it is classed as a Storm Sudden Commencement (SSC), if not then it is termed a Sudden Impulse (SI). Often such a classification is evaluated using the minimum observed values of the Dst or Sym-H indices (e.g. Joselyn & Tsurutani, 1990; Gonzalez et al., 1994; Turner et al., 2015; Curto et al., 2007; Fiori et al., 2014). In this work we designate an SC as an SSC if Sym-H drops below -50 nT in the 24 hours following the SC, and otherwise designate it as an SI. In total, 215 events meet the criteria and are classed as SSCs, which leaves 165 SIs. Historically, the distinction has also been made by considering whether the magnetic “rhythm” at the station changed character (e.g. Mayaud, 1973), however this is more difficult to perform in an automated and reproducible fashion, and so has not been applied. This scheme follows that used by Smith et al. (2019), and ensures that the results are directly comparable with that earlier study.

205

3 Results

206

3.1 Assessing the PDFs of R

207

208

209

Figure 2 shows Probability Density Functions (PDFs) of R for the 12 stations included in this study. Figure 2a shows the PDFs of R for the full dataset (1996 - 2016) and Figure 2b shows the PDF of R during SCs. Figure 2c shows the ratio of the PDFs

210 observed during SCs to the PDFs from the complete dataset, showing the relative like-
 211 lihood of a level of R during SCs compared to the dataset as a whole. The PDFs are binned
 212 using the method of Freeman et al. (2019), while the color indicates the magnetic lati-
 213 tude of the observatory.

214 For the full interval (Figure 2a), the PDFs show a clear ordering, with PDFs from
 215 stations at higher latitudes (i.e. those that are towards the red end of the color scale)
 216 showing higher probability densities at larger R when compared with those at lower ge-
 217 omagnetic latitudes (i.e. those towards the blue end of the color scale). This shift is most
 218 dramatic at mid to high latitudes, i.e. for stations with geomagnetic latitudes greater
 219 than $\sim 55^\circ$. For example, at an R of 10 nT min^{-1} the difference between the PDFs of
 220 stations near the magnetic equator (e.g. MBO) and those at $\sim 55^\circ$ (e.g. LER) is ap-
 221 proximately an order of magnitude, showing that R of this level is ~ 10 times more com-
 222 mon at the higher latitude station. Meanwhile, the difference between stations at $\sim 55^\circ$
 223 and those at $\sim 65^\circ$ (e.g. ABK) is also an order of magnitude, despite a much smaller
 224 latitudinal difference. This highlights the region at which the phenomena related to the
 225 auroral currents begin to exert a greater influence on the rate of change of the field (e.g.
 226 Rogers et al., 2020).

227 When we compare the PDFs obtained during SC intervals (Figure 2b) we find that
 228 they are shifted towards larger R , as seen for the entire dataset (seen in Figure 2a). Again,
 229 this effect appears to be more pronounced at higher latitudes, with a greater shift to larger
 230 values of R . As the SCs included are identical between stations, this suggests that larger
 231 values of R are observed at higher latitude stations during the same SC event, reflect-
 232 ing a form of high latitude enhancement (e.g. Fiori et al., 2014).

233 The ratio of the PDFs from the SCs to the PDFs from the entire dataset for each
 234 station are shown in Figure 2c. The dashed horizontal line indicates a ratio of 1. These
 235 ratios show that rates of change smaller than $\sim 1 - 10 \text{ nT min}^{-1}$ are less likely dur-
 236 ing SCs than at a randomly selected interval, while R larger than $\sim 1 - 10 \text{ nT min}^{-1}$
 237 are more likely to be observed. This transition was previously noted in a study of the
 238 subset of data from the UK based stations (Smith et al., 2019). The transition can be
 239 seen to vary with latitude. Lower latitude stations (e.g. below 50°) show this transition
 240 at values of $R \sim 1 \text{ nT min}^{-1}$, while higher latitude stations see it closer to 10 nT min^{-1} .
 241 It is also noteworthy that the ratio of the PDFs at significant R (e.g. $R > 10 \text{ nT min}^{-1}$)
 242 is much larger at lower latitude stations. For example, at low latitudes an R of 30 nT min^{-1}
 243 is approximately 700 times more likely to be observed during an SC than at any randomly
 244 selected interval. In contrast, at the highest latitude station (e.g. ABK), observations
 245 of $R = 30 \text{ nT min}^{-1}$ are only approximately seven times more likely during SCs. There-
 246 fore, while SCs are associated with larger R at higher latitudes, SCs are more likely to
 247 be associated with unusually large R at lower latitudes.

248 3.2 The Contribution of SCs

249 Smith et al. (2019) found that around 8% of observations of $R \geq \sim 50 \text{ nT min}^{-1}$
 250 were directly attributable to SCs for the HAD station at a magnetic latitude of 47.37° .
 251 To explore how this changes with latitude, Figure 3a shows the percentage of data ex-
 252 ceeding prescribed levels of R that can be directly related to SCs. The percentages are
 253 plotted for each of the 12 stations, with the color once again indicating the geomagnetic
 254 latitude of the station. It is clear from Figure 3a that SCs become responsible for an in-
 255 creasing percentage of extreme variation as the geomagnetic latitude of the station re-
 256 duces towards the equator. Above a level of $\sim 60 \text{ nT min}^{-1}$ up to 40% of the obser-
 257 vations are related directly to SCs at the lowest latitude stations. As latitude increases
 258 to approximately 45° this percentage decreases to 10–20%. For the stations at higher
 259 latitudes, e.g. above $\sim 60^\circ$, less than 1% of data above an R of 10s of nT min^{-1} is at-

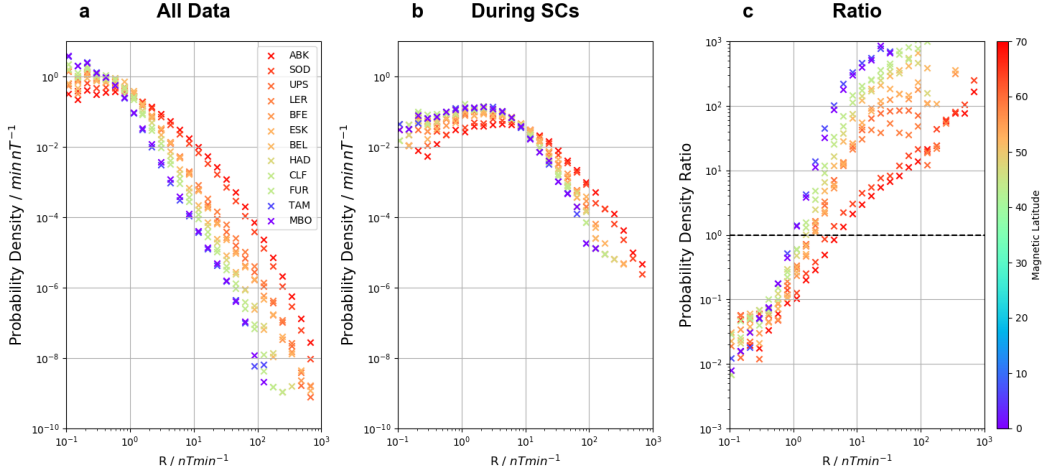


Figure 2. PDFs of R between 1996 and 2016 for the 12 magnetometer stations in Figure 1 and Table 1 (a), PDFs of R during 380 SC intervals for the same stations (b), and the ratio between the PDF during SCs and at all times (c). The color of the PDF is given by the magnetic latitude of the magnetometer station.

260 tributable to SCs. This again highlights the importance and significance of other phe-
 261 nomena at these latitudes.

262 Figures 3b and c are plotted in the same format as Figure 3a, however the SCs have
 263 been split into those classed as SSCs (Figure 3b) and SIs (Figure 3c). This classification
 264 has been performed on the basis of the Sym-H index in the 24 hours that follow the SC
 265 (see Section 2.2). It can be seen that Figure 3b closely resembles Figure 3a, such that
 266 the majority of the large rates of change can be attributed to the 215 SSCs. Figure 3c
 267 on the other hand, displaying the rates of change associated with SIs, shows a similar
 268 pattern but the percentages are about an order of magnitude lower. SIs can be seen to
 269 account for less than 2% of observations of elevated R even at the lowest latitudes. This
 270 suggests that the interplanetary shocks that create the most significant initial ground
 271 response are more likely to lead to further global magnetospheric activity, i.e. a geomag-
 272 netic storm.

273 3.2.1 Quantifying the Contribution Above $50 nT min^{-1}$

274 We now look to quantitatively evaluate how the fraction of large R attributable to
 275 SCs changes with latitude, and how the days that follow the SC contribute to that frac-
 276 tion of R . Figure 4 shows how the percentage of data above $50 nT min^{-1}$ related to SCs
 277 varies as a function of magnetic latitude. Effectively, Figure 4 shows vertical slices through
 278 Figure 3 at $R = 50 nT min^{-1}$. The $50 nT min^{-1}$ threshold has been selected as it rep-
 279 resents a large rate of change at all stations, yet retaining sufficient data at all latitudes.
 280 The impact of changing this threshold will be assessed in Section 3.2.2. Inspecting the
 281 top row of Figure 4 we see that an increasing percentage of data above $50 nT min^{-1}$ is
 282 attributable to SCs as magnetic latitude decreases, leading to a maximum of $\sim 32\%$ at
 283 the lowest latitude station. Specifically, the $50 nT min^{-1}$ threshold was broken on 12
 284 occasions during SCs (during 11 separate events), out of a total of 38 total intervals above
 285 $50 nT min^{-1}$. Meanwhile, above a geomagnetic latitude of approximately 50° the equiv-
 286 alent percentage is very small ($\leq 1\%$). Comparing SSCs and SIs (Figures 4b i and c i)
 287 we again find that SIs are responsible for less than 1% of instances of R exceeding $50 nT min^{-1}$
 288 at any latitude.

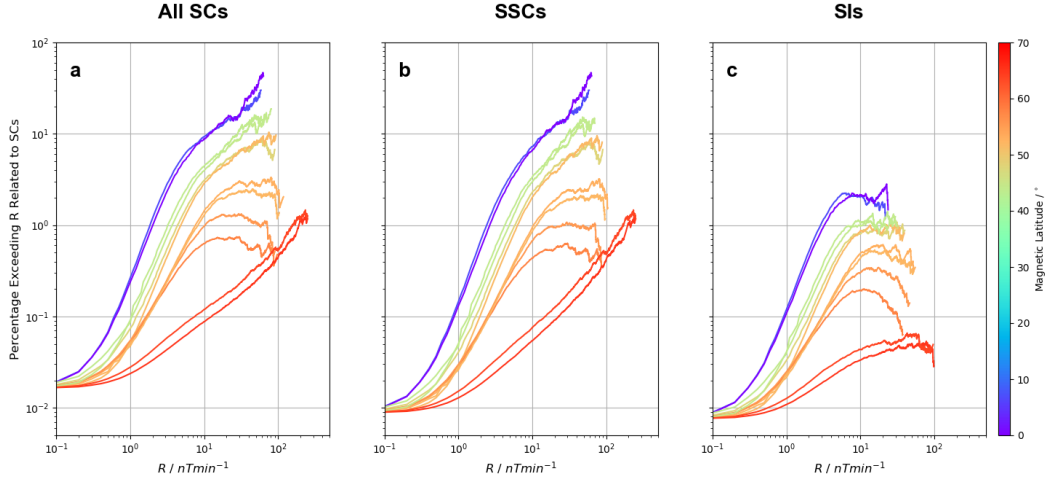


Figure 3. The percentage of data (1996 - 2016) exceeding a given level of R that is related to SCs. The results for each of the 12 stations are plotted, with the color representing the magnetic latitude of the station. The curves are shown for all 380 SCs (a), 215 SSCs (b) and 165 SIs (c), as defined in Section 2.2. The lines/percentages for each station are truncated where less than five positive instances remain in order to remove variability at large R related to a small number statistics.

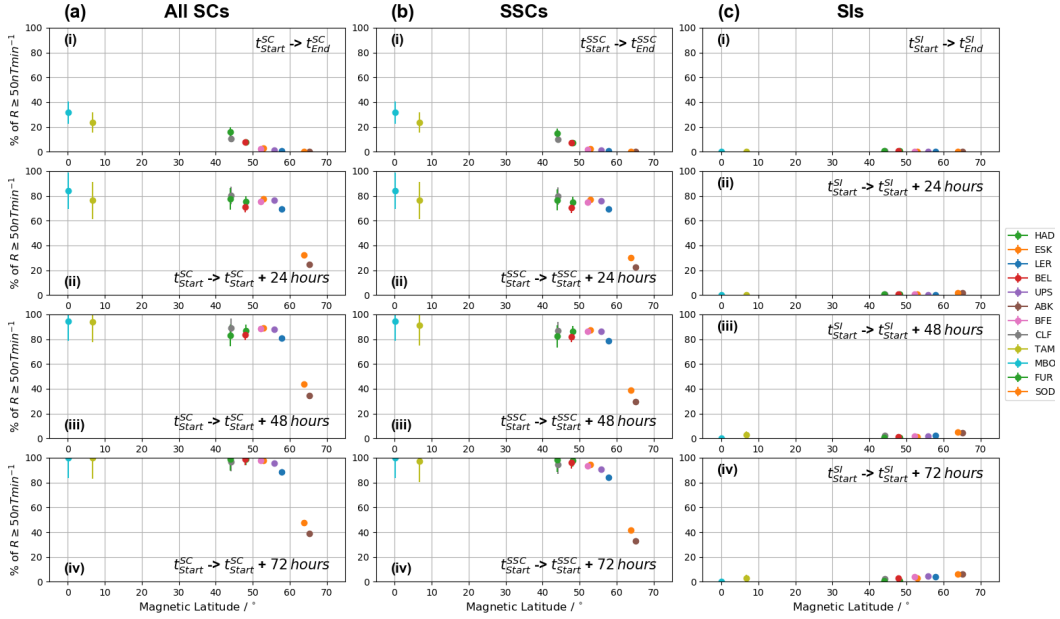


Figure 4. The percentage of observations of $R \geq 50 \text{ nT min}^{-1}$ that can be related to SCs as a function of magnetic latitude. The columns are plotted for (a) all 380 SCs, (b) 215 SSCs and (c) 165 SIs. The rows represent the data obtained during the SCs themselves (i), then the data inclusive of 24, 48 and 72 hours following the SC (ii, iii, and iv respectively).

289 When we include the data obtained in the 24 hours that follows an SC (Figure 4a
 290 ii) we see that below a latitude of 60° about 75% of R exceeding 50 nT min^{-1} occurs
 291 during this interval, rising to 80 – 90% at the lowest latitude stations. Above a mag-
 292 netic latitude of 60° this percentage is below 50%. As with the data from the SCs them-
 293 selves, when we subdivide the SCs by type (Figures 4 b ii and c ii) we find that the pe-
 294 riod 24 hours following SIs accounts for less than 1% of the R exceeding 50 nT min^{-1} .

295 Including the second and third days after the SCs increases the percentage of $R \geq$
 296 50 nT min^{-1} that can be explained incrementally, by approximately 10–20% per ad-
 297 ditional day included (e.g. moving from Figure 4a iii to iv). For stations at latitudes lower
 298 than 60° , 90–100% of all R exceeding 50 nT min^{-1} occurred within three days of an
 299 SC. In contrast, above 60° the percentage is still below $\sim 50\%$. Mirroring the results
 300 in Figure 3, when splitting the SCs into SSCs and SIs, we find that SSC related inter-
 301 vals account for almost all of the $R \geq 50 \text{ nT min}^{-1}$, while SIs and the related inter-
 302 vals account for $< 5\%$ at all latitudes.

303 We note that 87 of the SCs occur within the three day interval following a previ-
 304 ous SC. For these events the rates of change of the field are included in the statistics of
 305 the most recent SC, and are not double counted.

3.2.2 *Evaluating the Contribution as a Function of Threshold*

307 In the above we considered the contribution of SCs to rates of change above a fixed
 308 threshold of 50 nT min^{-1} . We now examine how adjusting this R threshold impacts how
 309 the contribution of SCs changes with latitude. Figures 5a and b show how this percent-
 310 age varies for SCs and SCs + 1 day (i.e. in the first 24 hours), respectively. Panels i to
 311 vii in Figure 5 show the results for thresholds between 10 to 70 nT min^{-1} , in increments
 312 of 10 nT min^{-1} . First, considering just the data during SCs themselves (Figure 5a), as
 313 the threshold increases we see that the fraction of R attributable to SCs increases. This
 314 trend can also be seen in Figure 3. Above 10 nT min^{-1} (Figure 5a i) at the most equa-
 315 torial station $\sim 10\%$ of the data is directly related to SCs, while by the time the thresh-
 316 old is set to 70 nT min^{-1} this increases to around 35%. However, it is also clear that
 317 this increase in percentage is mostly concentrated at lower latitudes, and that above \sim
 318 50° geomagnetic latitude the increase is relatively minor.

319 When we include the data that occurred in the day that follows an SC, i.e. inspect-
 320 ing Figures 5b i to vii, we find that the percentage attributable to this SC related inter-
 321 val is relatively constant with increasing threshold. Over a threshold of $\sim 20 \text{ nT min}^{-1}$,
 322 it plateaus at approximately 70–80% for most latitudes. Above 60° however, a smaller
 323 percentage is attributable to SCs and the following 24 hours of observations. For these
 324 high latitude stations, above 10 nT min^{-1} around 15% of data is explained, which in-
 325 creases to around 25 – 30% at levels above 70 nT min^{-1} .

326 The red lines in Figure 5 represent simple linear fits to the results from stations
 327 below 55° magnetic latitude. The fitting limit of 55° was determined manually from in-
 328 spection, where stations above this latitude have results that appear significantly differ-
 329 ent. This linear fit can be seen to well to capture most of the trends, particularly in Fig-
 330 ure 5a (during SCs). The parameters of these empirical fits are shown in Figure 6.

331 In Figure 6a, which shows the results for the SC intervals, we see that the gradi-
 332 ent of the fit increases as the threshold of R increases. Further, this same pattern is seen
 333 in the intercept (Figure 6c), which is equivalent to the equatorial projection of the per-
 334 centage contribution of SCs, assuming a linear fit to the stations below 55° . This equa-
 335 torial percentage increases from $\sim 10\%$ at a limit of 10 nT min^{-1} , exceeding a fraction
 336 of $\sim 40\%$ above an $R \sim 50 \text{ nT min}^{-1}$, albeit with considerable uncertainty at the higher
 337 thresholds. This combination of increasing gradient and intercept with threshold sug-

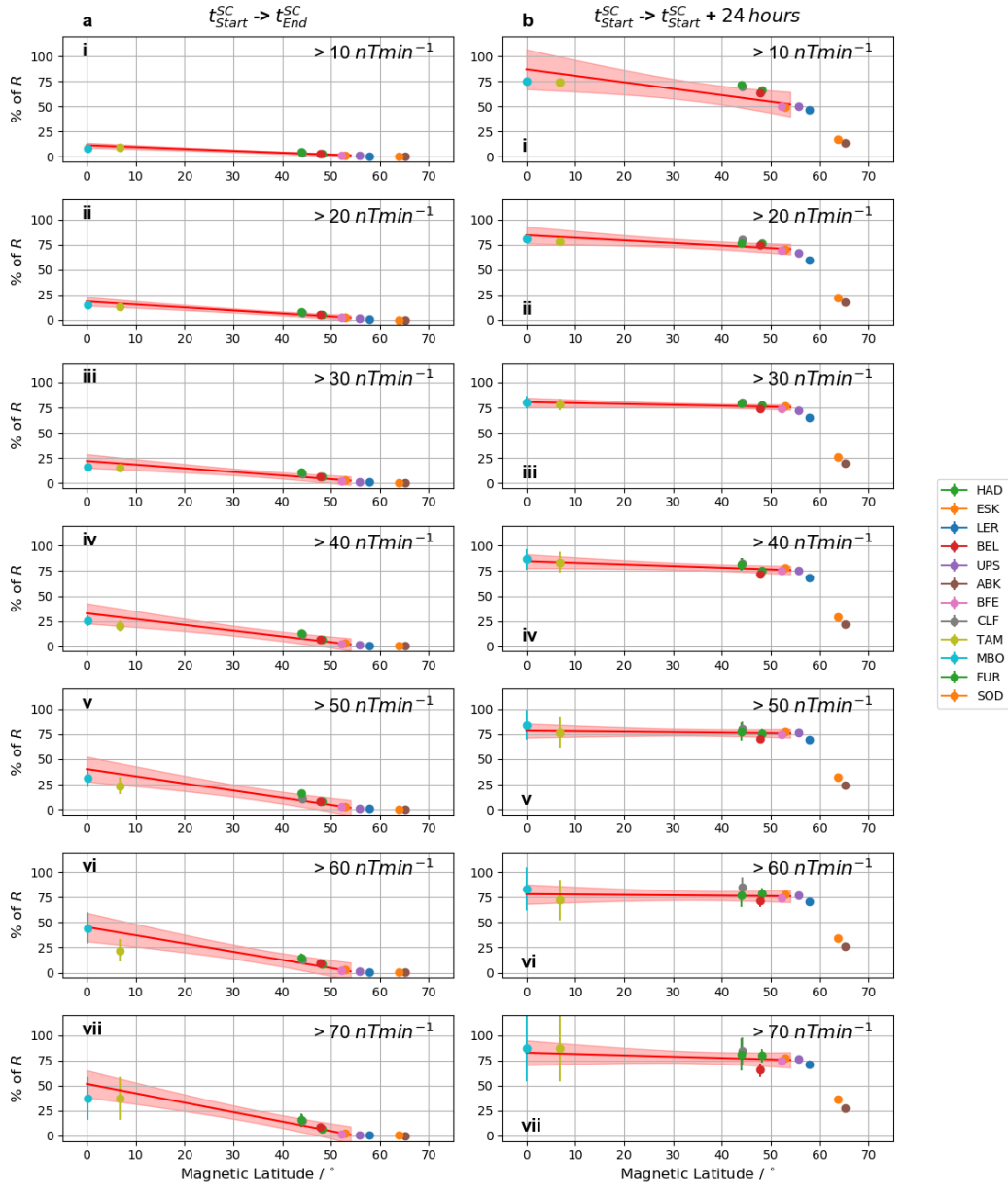


Figure 5. The fraction of data exceeding given values of R that can be related to SCs as a function of magnetic latitude, for increasing thresholds of R in panels i to iv. The threshold ranges from 10 nT min^{-1} (i) to 70 nT min^{-1} (vii) in steps of 10 nT min^{-1} . The columns are plotted for all 380 SCs (a) and all 380 SCs including the 24 hours that follow (b). The red line indicates the results of a linear fit to stations at less than 55° magnetic latitude. The red shaded region indicates the 95% confidence interval from the linear fitting procedure.

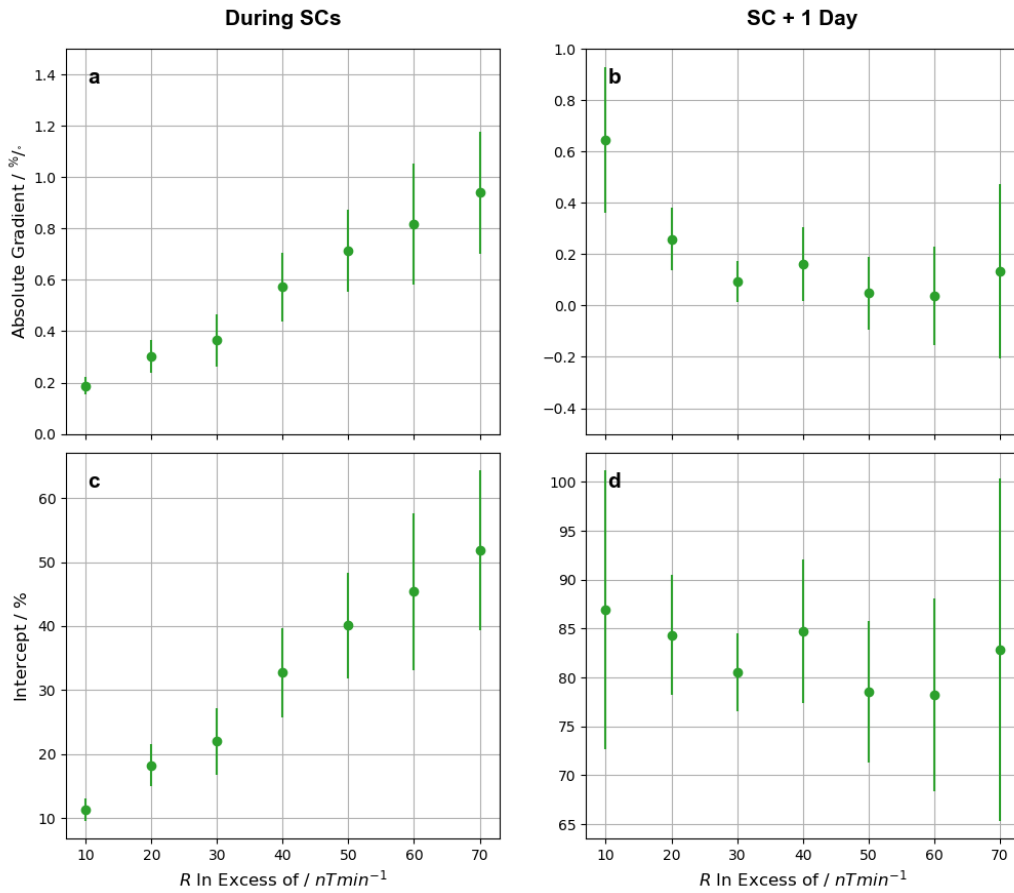


Figure 6. The results of the linear fits to Figure 5, below a latitude of 55° . The absolute value of the linear best fit gradient for SCs and SCs plus 1 day, respectively (a and b). The value of the intercept at the magnetic equator, once more for SCs and SCs plus 1 day (c and d). The error bars indicate the 1σ uncertainty in the least squares fit, calculated from the covariance matrix.

gest that while SCs do become more important at higher thresholds at all latitudes, this increase is greatest at the lowest latitudes.

Considering the results for SCs and the day that follows, Figure 4b and d, we see that the gradient decreases and flattens to zero as the R threshold increases, while the intercept remains relatively constant. Nonetheless, the intercept appears between 75% and 90%, suggesting that, within uncertainties the vast majority of $R \geq 10 \text{ nT min}^{-1}$ at low latitudes is found within a day of an SC. Further, due to the small gradients obtained, this result is widely applicable to locations with magnetic latitudes below 55° .

4 Discussion

In this work we have evaluated the contribution of SCs to large rates of change of the ground magnetic field as a function of latitude, using an array of 12 magnetometer stations across Europe and North Africa. Our results show that while SCs are larger at higher geomagnetic latitudes, they form a larger fraction of extreme magnetic field variability at lower latitudes. Further, only SSC type events cause significant magnetic field variability and below 60° magnetic latitude the three days that follow an SSC contribute the vast majority of R above 50 nT min^{-1} .

4.1 Latitudinal Variation of SC Risk

We examined how the PDFs of R change with geomagnetic latitude (Figure 2), comparing and contrasting the complete data set with that obtained during SC-related intervals. We showed that higher latitude stations show PDFs that are shifted towards larger values of R , both during SCs and in the full data set. SCs have been observed to present with larger rates of change of the field at higher magnetic latitudes, and this has been linked to ionospheric current systems that are only generated at such locations (e.g. Araki, 1994; Fiori et al., 2014). While the magnitude of SCs is lower closer to equatorial latitudes, we also showed that they represent intervals during which rates of change of around 30 nT min^{-1} are up to 700 times more likely than during any random interval. This relative likelihood is smaller at higher latitudes, being of the order of 10 times more likely. As the rate of change (R) increases, SCs contribute an even greater percentage of the data at low latitudes. This demonstrates how at lower latitudes there are fewer phenomena that can generate large rates of change of the field. Meanwhile, at higher latitudes other magnetospheric processes, such as storms, substorms, and convection can be inferred to control the majority of significant R (e.g. Freeman et al., 2019).

We have also shown that the importance of the period that follows SCs is considerable, with the first day post-SC accounting for around 85% of variability exceeding 20 nT min^{-1} , below a latitude of 55° . While this does not change significantly as the latitude increases from the equator, there is a considerable jump at around $55 - 60^\circ$ magnetic latitude, above which SCs and the days that follow only contribute a dramatically $\sim 30\%$ of the large values of R , at all thresholds tested. This corresponds to the region in which the auroral currents most often reside (Thomson et al., 2011; Rogers et al., 2020). This is not to say that SCs don't have an impact at these latitudes, but they are a part of a plethora of geomagnetic activity that can result in large magnetic perturbations at the ground.

4.2 Link to GICs: Comparison with New Zealand

Large GICs have been directly measured during SCs and during magnetospheric activity that follows (e.g. Pulkkinen et al., 2005; Rodger et al., 2017). Clilverd et al. (2018) performed a detailed study of the September 2017 geomagnetic storm, using observations of the local magnetic field variability and GICs in New Zealand and noted that each of the two interplanetary shock impacts in the interval studied were associated with enhanced variability in the field and GICs. They also found that both of these SCs were followed

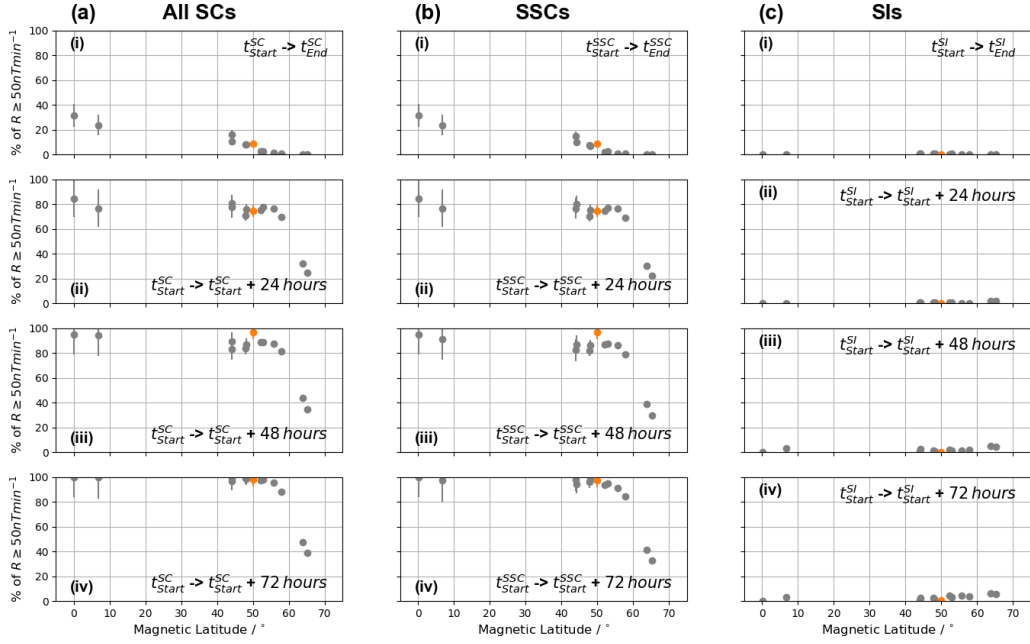


Figure 7. The percentage of $R \geq 50 \text{ nT min}^{-1}$ that can be related to SCs as a function of magnetic latitude. The format is as in Figure 4, with the 12 stations in Table 1 shown in gray and the EYR station in orange.

386 a few hours later by a second interval of elevated field variability and considerable GIC
 387 probably associated with substorms. Our study corroborates these results and places them
 388 in the context of observations from a large historical dataset of ground magnetic field
 389 rates of change, showing that the largest amplitude variations occur within the period
 390 following SSCs. However, we lack direct and contemporaneous observations of GICs for
 391 the European and North African locations included in the current study. It is therefore
 392 instructive to compare our statistical geomagnetic field variability results from the north-
 393 ern hemisphere with New Zealand, where direct GIC measurements are available and strong
 394 correlations between SCs and related magnetospheric activity and GICs have been ob-
 395 served.

396 Figure 7 shows the percentage of data for which $R \geq 50 \text{ nT min}^{-1}$ that is asso-
 397 ciated with SCs as a function of magnetic latitude. The format is the same as in Fig-
 398 ure 4, but with the twelve stations originally included in this study now plotted in gray.
 399 The EYR INTERMAGNET station, located at Eyrewell in New Zealand at a magnetic
 400 latitude of -50° and longitude of -103.64° , is included in orange at its conjugate lat-
 401 itude.

402 The results from EYR are consistent with the previously noted trends from the north-
 403 ern hemisphere stations. We note that the original station selection process (Section 2)
 404 required that the stations were as close together in longitude as possible, in order to mit-
 405 igate any local time effects. This consistency between the north and south results indi-
 406 cates that the local time differences that prompted the longitudinal constraints imposed
 407 in our station selection are relatively minor over the long statistical time period consid-
 408 ered in this work. This suggests that the results we report are likely more broadly ap-
 409 plicable rather than being restricted to the longitude range of stations shown in Figure
 410 1. This also suggests that the close associations noted between GICs and SCs (and fol-
 411 lowing intervals) in New Zealand may also be present in other locations if such direct

GIC measurements were available. However, we note that while the statistical analysis of the rate of change of the magnetic field is consistent between these locations, the relationship between magnetic fluctuations and GIC depends strongly on the orientation of the power network, its internal connectivity and resistivity, and local geology (e.g. Thomson et al., 2005; Beggan, 2015; Divett et al., 2018).

It is also interesting to note that although we have considered the initial SC impact and the magnetospheric activity in the days that follow as a whole (e.g. storms and substorms), distinct phenomena may have slightly different implications for power networks. Part of this will be due to the orientation of the variability, for example SCs are predominantly in the northward direction which would couple differently to a given power network than an east-west deflection. Second, different phenomena will operate over different timescales, which may present a different hazard to a given system (e.g. Clilverd et al., 2020). The different effects of the distinct phenomena were noted by Clilverd et al. (2018), who found that while SSCs and later periods both resulted in the generation of significant GICs in the power network, only the longer lasting post-SC intervals were related to the generation of harmonics in the power network. This kind of consideration would be of key importance to the use of forecasts of SCs in the operation of power networks.

It is also important to note that this study has concerned the results obtained with one-minute resolution magnetic field data, which have been shown to correlate well with observed GICs (e.g. Mac Manus et al., 2017; Rodger et al., 2017). Yet SCs often represent very fast magnetic fluctuations that may not be adequately captured by one-minute resolution data (e.g. Araki, 2014). For this reason, it may be that SCs are more important when the rates of change of higher resolution magnetic field data are considered. However, we note that due to smoothing effects from the local ground conductivity and network inductance, high frequency magnetic fluctuations do not necessarily translate directly to significant GICs (e.g. Divett et al., 2018; Clilverd et al., 2020).

4.3 Forecasting Large Geomagnetic Field Fluctuations

From the perspective of mitigating the risks posed by GICs, it is of great importance to be able to forecast intervals in which they might be generated. Until recently, there had been little success at forecasting substorms, and therefore the substorm-driven GICs with which they are associated. It had been shown that their recurrence and amplitude could be predicted statistically, but not for individual events (Freeman & Morley, 2004; S. K. Morley & Freeman, 2007). Recently however, Maimaiti et al. (2019) showed that machine learning methods can be used to predict substorms 75% of the time. Nevertheless the solar wind driving between substorm and non-substorm intervals showed strong similarities, testifying to the difficulty of forecasting such a phenomenon purely on the basis of the external solar wind.

Looking to forecasting other significant phenomena, approximately 75% of SCs are preceded by the observation of an interplanetary shock upstream of the Earth at L1 (Wang et al., 2006; Smith et al., 2020), providing a significant amount of warning and the opportunity to forecast the consequences of the shock. Excellent correlations have historically been observed between large geomagnetic storms and interplanetary shocks (Chao & Lepping, 1974; Gosling et al., 1991); while statistically between ~ 45 and 60% of interplanetary shocks incident at the Earth being linked to geomagnetic storm activity in the days that follow (Echer & Gonzalez, 2004).

The SCs studied in this work have been broken down by whether they were followed by further significant geomagnetic activity, i.e. a geomagnetic storm. Those that are can be termed an Storm Sudden Commencement (SSC), while those that are not can be called a Sudden Impulse (SI) (e.g. Joselyn & Tsurutani, 1990; Curto et al., 2007). Recent modeling efforts have shown good skill and reliability in distinguishing between interplan-

etary shocks likely to result in SSCs or SIs in advance (Smith et al., 2020). When we make such a distinction, we found that SI-type events are not related to substantial fractions of enhanced R . In contrast, the substantial fractions of enhanced R observed during the full complement of SCs (or in the days that follow) are solely due to those events that have been classed as SSCs. Therefore, being able to make this distinction would help to narrow consideration of intervals during which large R may be observed.

Our results confirm the critically important contribution of SSCs to low-to-mid latitude magnetic field perturbations (e.g. Carter et al., 2015; Marshall et al., 2012). They suggest that for the lowest latitudes SSCs are one of the dominant processes that can generate large R , and consequently large GIC. At equatorial magnetic latitudes, the ability to forecast SSCs would allow a 24 hour window to be identified which would account for over 80% of rates of change of the magnetic field greater than 70 nT min^{-1} . Meanwhile at mid latitudes, as with the preliminary work of Smith et al. (2019), we have found that the days that follow SSCs contribute strongly to values of R exceeding 50 nT min^{-1} . Over 90% of such values of R are recorded within three days of an SSC for stations below $\sim 55 - 60^\circ$. Therefore, observations upstream of the Earth allow for a broad window of warning that such large R may occur in the next few days at mid-low latitudes. Such a warning could be exploited by the energy transmission industry, applying mitigation approaches over that time window.

These results also have consequences for the horizon with which large rates of the change can be forecast. Without the use of heliospheric imagery or models (e.g. Odstrcil, 2003; Davies et al., 2012, 2013; M. J. Owens & Riley, 2017; L. A. Barnard et al., 2019; L. Barnard et al., 2020; M. Owens et al., 2020), the large rates of change of the field caused by an interplanetary shock impact (i.e. an SC) may be, at most, forecast by the travel time between the observations at L1 and the Earth's magnetopause: likely less than an hour. Therefore, at the lowest latitudes around 25–35% of large rates of change of the field may only be forecast with a maximum of an hour lead time. On the other hand, the very large fraction of mid-low latitude rates of change observed in the days that follow an SC may be forecast with a longer lead time, though imprecisely.

At high geomagnetic latitudes, here defined to be around $\sim 55 - 60^\circ$, the relative importance of other phenomena was shown to increase such that $\leq 50\%$ of R exceeding 50 nT min^{-1} is found within three days of an SSC. At these latitudes it is likely that forecasting phenomena outside of geomagnetic storms such as substorms is a critical process (e.g. Maimaiti et al., 2019). Such forecasting would also provide a more precise window of warning, of the order of an hour, rather than the days provided by consideration of SSCs and related activity.

5 Summary

In this work we have assessed the contribution of Sudden Commencements to large rates of change of the horizontal magnetic field (R), exploring this as a function of latitude and level of variability. In general, large rates of the change of the magnetic field would be expected to drive large GICs, which may pose a risk to the operation of power networks.

We have shown that the relative importance of SCs producing high R increases moving towards the equator, and that at the lowest latitudes during an SC magnetic fluctuations around 30 nT min^{-1} are around 700 times more likely than in any random interval. In contrast, by a latitude of $\sim 65^\circ$ this factor drops to less than 10 times more likely.

We have shown that SCs represent over 25% of geomagnetic field fluctuations above 50 nT min^{-1} at the lowest latitudes. Again, this drops off as latitude increases to $\leq 1\%$ by $\sim 55^\circ$. If we include the three day interval following an SC, we can account for greater

513 than 90% of field fluctuations above 50 nT min^{-1} below a magnetic latitude of $\sim 60^\circ$.
 514 Above this latitude other phenomena that may be unrelated to SCs, such as non-storm
 515 time isolated substorms, account for the majority of magnetic perturbations.

516 Critically, we have also shown that the elevated values of R associated with SCs
 517 are almost entirely due to the subset of SCs that are followed by a geomagnetic storm,
 518 termed SSCs. This is observed both for the case of immediate large R , and also for the
 519 few days that follow.

520 This work has quantified the impact of SCs, and confirmed their significance for
 521 mid-low latitude magnetic field changes, both directly and also as an indication that sig-
 522 nificant geomagnetic activity may follow. This has important consequences for the fore-
 523 casting of large rates of change of the geomagnetic field, and consequent GICs.

524 Acknowledgments

525 The results presented in this paper rely on data collected at magnetic observatories. We
 526 thank the national institutes that support them and INTERMAGNET for promoting
 527 high standards of magnetic observatory practice (www.intermagnet.org). The data were
 528 downloaded from <https://intermagnet.github.io> and are freely available there.

529 The results presented in the paper also rely on the SC list made available by the
 530 International Service on Rapid Magnetic Variations (<http://www.obsebre.es/en/rapid>)
 531 and published by the Observatorio de l'Ebre in association with the International As-
 532 sociation of Geomagnetism and Aeronomy (IAGA) and the International Service of Ge-
 533 omagnetic Indices (ISGI). We thank the involved national institutes, the INTERMAG-
 534 NET network and the ISGI.

535 AWS and IJR were supported by STFC Consolidated Grant ST/S000240/1, and
 536 NERC grants NE/P017150/1 and NE/V002724/1. CF was supported by the NERC In-
 537 dependent Research Fellowship NE/N014480/1, NERC grant NE/V002724/1 and STFC
 538 Consolidated Grant ST/S000240/1. CJR was supported by the New Zealand Ministry
 539 of Business, Innovation & Employment through Endeavour Fund Research Programme
 540 contract UOOX2002. MPF was supported by NERC grants NE/P016693/1 (SWIGS)
 541 and NE/V002716/1 (SWIMMR SAGE).

542 The analysis in this paper was performed using python, including the pandas (McKinney,
 543 2010), numpy (Van Der Walt et al., 2011), scikit-learn (Pedregosa et al., 2011), scipy (Virtanen
 544 et al., 2020) and matplotlib (Hunter, 2007) libraries.

545 References

- 546 Akasofu, S.-I. (1964). The development of the auroral substorm. *Plane-*
 547 *tary and Space Science*, *12*(4), 273–282. Retrieved from [http://www](http://www.sciencedirect.com/science/article/pii/0032063364901515%5Cnhttp://linkinghub.elsevier.com/retrieve/pii/0032063364901515)
 548 [.sciencedirect.com/science/article/pii/0032063364901515%5Cnhttp://](http://www.sciencedirect.com/science/article/pii/0032063364901515%5Cnhttp://linkinghub.elsevier.com/retrieve/pii/0032063364901515)
 549 linkinghub.elsevier.com/retrieve/pii/0032063364901515 doi:
 550 10.1016/0032-0633(64)90151-5
- 551 Akasofu, S.-I., & Chao, J. (1980, apr). Interplanetary shock waves and magne-
 552 tospheric substorms. *Planetary and Space Science*, *28*(4), 381–385. Re-
 553 trieved from [https://www.sciencedirect.com/science/article/pii/](https://www.sciencedirect.com/science/article/pii/0032063380900422?via%3Dihub)
 554 [0032063380900422?via%3Dihub](https://www.sciencedirect.com/science/article/pii/0032063380900422?via%3Dihub) doi: 10.1016/0032-0633(80)90042-2
- 555 Araki, T. (1977, apr). Global structure of geomagnetic sudden commence-
 556 ments. *Planetary and Space Science*, *25*(4), 373–384. Retrieved from
 557 <https://www.sciencedirect.com/science/article/pii/0032063377900538>
 558 doi: 10.1016/0032-0633(77)90053-8
- 559 Araki, T. (1994, jan). A Physical Model of the Geomagnetic Sudden Commence-
 560 ment. In M. Engebretson, K. Takahashi, & M. Scholer (Eds.), *Solar wind*

- 561 *sources of magnetospheric ultra-low-frequency waves* (p. 183).
- 562 Araki, T. (2014, dec). Historically largest geomagnetic sudden commencement
563 (SC) since 1868. *Earth, Planets and Space*, 66(1), 164. Retrieved from
564 [https://earth-planets-space.springeropen.com/articles/10.1186/
565 s40623-014-0164-0](https://earth-planets-space.springeropen.com/articles/10.1186/s40623-014-0164-0) doi: 10.1186/s40623-014-0164-0
- 566 Araki, T., Fujitani, S., Emoto, M., Yumoto, K., Shiokawa, K., Ichinose, T., ... Liu,
567 C. F. (1997, jan). Anomalous sudden commencement on March 24, 1991. *Jour-
568 nal of Geophysical Research: Space Physics*, 102(A7), 14075–14086. Retrieved
569 from <http://doi.wiley.com/10.1029/96JA03637> doi: 10.1029/96JA03637
- 570 Barnard, L., Owens, M. J., Scott, C. J., & Koning, C. A. (2020, sep). Ensemble
571 CME Modeling Constrained by Heliospheric Imager Observations. *AGU Ad-
572 vances*, 1(3), e2020AV000214. Retrieved from [https://onlinelibrary.wiley
573 .com/doi/10.1029/2020AV000214](https://onlinelibrary.wiley.com/doi/10.1029/2020AV000214) doi: 10.1029/2020AV000214
- 574 Barnard, L. A., Owens, M. J., Scott, C. J., & Jones, S. R. (2019, jun). Extract-
575 ing Inner-Heliosphere Solar Wind Speed Information From Heliospheric
576 Imager Observations. *Space Weather*, 17(6), 925–938. Retrieved from
577 <https://onlinelibrary.wiley.com/doi/abs/10.1029/2019SW002226> doi:
578 10.1029/2019SW002226
- 579 Bedrosian, P. A., & Love, J. J. (2015, dec). Mapping geoelectric fields during
580 magnetic storms: Synthetic analysis of empirical United States impedances.
581 *Geophysical Research Letters*, 42(23), 10160–10170. Retrieved from
582 <https://onlinelibrary.wiley.com/doi/abs/10.1002/2015GL066636> doi:
583 10.1002/2015GL066636
- 584 Began, C. D. (2015, dec). Sensitivity of geomagnetically induced currents to vary-
585 ing auroral electrojet and conductivity models. *Earth, Planets and Space*,
586 67(1), 24. Retrieved from [http://www.earth-planets-space.com/content/
587 67/1/24](http://www.earth-planets-space.com/content/67/1/24) doi: 10.1186/s40623-014-0168-9
- 588 Beland, J., & Small, K. (2004). Space weather effects on power transmission sys-
589 tems: The cases of Hydro-Quebec and transpower NewZealand Ltd [Pro-
590 ceedings Paper]. In I. Daglis (Ed.), *Effects of space weather on technology
591 infrastructure* (Vol. 176, pp. 287–299). PO BOX 17, 3300 AA DORDRECHT,
592 NETHERLANDS: SPRINGER.
- 593 Borovsky, J. E., & Denton, M. H. (2006, jul). Differences between CME-driven
594 storms and CIR-driven storms. *Journal of Geophysical Research: Space
595 Physics*, 111(A7). Retrieved from [https://agupubs.onlinelibrary.wiley
596 .com/doi/full/10.1029/2005JA011447](https://agupubs.onlinelibrary.wiley.com/doi/full/10.1029/2005JA011447) doi: 10.1029/2005JA011447
597 -9402.SOLARWIND1 doi: 10.1029/2005JA011447@10.1002/(ISSN)2169-9402
598 .SOLARWIND1
- 599 Boteler, D. H., Pirjola, R. J., & Nevanlinna, H. (1998, jan). The effects of geo-
600 magnetic disturbances on electrical systems at the Earth’s surface. *Advances in
601 Space Research*, 22(1), 17–27. Retrieved from [http://linkinghub.elsevier
602 .com/retrieve/pii/S027311779701096X](http://linkinghub.elsevier.com/retrieve/pii/S027311779701096X) doi: 10.1016/S0273-1177(97)01096
603 -X
- 604 Campbell, W. H. (1980, may). Observation of electric currents in the Alaska oil
605 pipeline resulting from auroral electrojet current sources. *Geophysical Journal
606 International*, 61(2), 437–449. Retrieved from [https://academic.oup.com/
607 gji/article-lookup/doi/10.1111/j.1365-246X.1980.tb04325.x](https://academic.oup.com/gji/article-lookup/doi/10.1111/j.1365-246X.1980.tb04325.x) doi: 10
608 .1111/j.1365-246X.1980.tb04325.x
- 609 Carter, B. A., Pradipta, R., Zhang, K., Yizengaw, E., Halford, A. J., & Norman,
610 R. (2015). Interplanetary shocks and the resulting geomagnetically induced
611 currents at the equator. *Geophysical Research Letters*, 42(16), 6554–6559.
612 Retrieved from [https://agupubs.onlinelibrary.wiley.com/doi/pdf/
613 10.1002/2015GL065060](https://agupubs.onlinelibrary.wiley.com/doi/pdf/10.1002/2015GL065060) doi: 10.1002/2015gl065060
- 614 Chao, J. K., & Lepping, R. P. (1974, may). A correlative study of ssc’s, interplane-
615 tary shocks, and solar activity. *Journal of Geophysical Research*, 79(13), 1799–

1807. Retrieved from <http://doi.wiley.com/10.1029/JA079i013p01799>
doi: 10.1029/JA079i013p01799
- Chree, C. (1925, jan). The times of "Sudden Commencements" (S.C.s) of magnetic storms: Observation and theory. *Proceedings of the Physical Society of London*, 38(1), 35–46. Retrieved from <http://stacks.iop.org/1478-7814/38/i=1/a=305?key=crossref.ddd5862873bdd55549f24a7b09002eda> doi: 10.1088/1478-7814/38/1/305
- Clilverd, M. A., Rodger, C. J., Brundell, J. B., Dalzell, M., Martin, I., Mac Manus, D. H., ... Obana, Y. (2018, jun). Long-Lasting Geomagnetically Induced Currents and Harmonic Distortion Observed in New Zealand During the 7-8 September 2017 Disturbed Period. *Space Weather*, 16(6), 704–717. Retrieved from <http://doi.wiley.com/10.1029/2018SW001822> doi: 10.1029/2018SW001822
- Clilverd, M. A., Rodger, C. J., Brundell, J. B., Dalzell, M., Martin, I., Mac Manus, D. H., & Thomson, N. R. (2020, oct). Geomagnetically Induced Currents and Harmonic Distortion: High time Resolution Case Studies. *Space Weather*. Retrieved from <https://onlinelibrary.wiley.com/doi/10.1029/2020SW002594> doi: 10.1029/2020SW002594
- Committee on the Peaceful Uses of Outer Space (COPUOS). (2017). *Thematic priority 4. International framework for space weather services* (Tech. Rep.). Retrieved from <http://www.unoosa.org/oosa/oosadoc/data/documents/2018/aac.105/aac.1051171.0.html> doi: A/AC.105/1171
- Coxon, J. C., Shore, R. M., Freeman, M. P., Fear, R. C., Browett, S. D., Smith, A. W., ... Anderson, B. J. (2019, jul). Timescales of Birkeland Currents Driven by the IMF. *Geophysical Research Letters*, 46(14), 7893–7901. Retrieved from <https://onlinelibrary.wiley.com/doi/10.1029/2018GL081658> doi: 10.1029/2018GL081658
- Curto, J. J., Araki, T., & Alberca, L. F. (2007, nov). Evolution of the concept of Sudden Storm Commencements and their operative identification. *Earth, Planets and Space*, 59(11), i–xii. Retrieved from <http://earth-planets-space.springeropen.com/articles/10.1186/BF03352059> doi: 10.1186/BF03352059
- Davies, J. A., Harrison, R. A., Perry, C. H., Möstl, C., Lugaz, N., Rollett, T., ... Savani, N. P. (2012, may). A SELF-SIMILAR EXPANSION MODEL FOR USE IN SOLAR WIND TRANSIENT PROPAGATION STUDIES. *The Astrophysical Journal*, 750(1), 23. Retrieved from <http://stacks.iop.org/0004-637X/750/i=1/a=23?key=crossref.89fa5eee2bfa06216666d60a43e23416> doi: 10.1088/0004-637X/750/1/23
- Davies, J. A., Perry, C. H., Trines, R. M. G. M., Harrison, R. A., Lugaz, N., Möstl, C., ... Steed, K. (2013, oct). ESTABLISHING A STEREO SCOPIC TECHNIQUE FOR DETERMINING THE KINEMATIC PROPERTIES OF SOLAR WIND TRANSIENTS BASED ON A GENERALIZED SELF-SIMILARLY EXPANDING CIRCULAR GEOMETRY. *The Astrophysical Journal*, 777(2), 167. Retrieved from <http://stacks.iop.org/0004-637X/777/i=2/a=167?key=crossref.bd1e7950fad53baa7c2f9d1ccbf3b988> doi: 10.1088/0004-637X/777/2/167
- Dimmock, A., Rosenqvist, L., Hall, J., Viljanen, A., Yordanova, E., Honkonen, I., ... Sjöberg, E. (2019, jun). The GIC and geomagnetic response over Fennoscandia to the 7th September 2017 geomagnetic storm. *Space Weather*, 2018SW002132. Retrieved from <https://onlinelibrary.wiley.com/doi/abs/10.1029/2018SW002132> doi: 10.1029/2018SW002132
- Dimmock, A. P., Rosenqvist, L., Welling, D., Viljanen, A., Honkonen, I., Boynton, R. J., & Yordanova, E. (2020, jun). On the regional variability of dB/dt and its significance to GIC. *Space Weather*. Retrieved from <https://onlinelibrary.wiley.com/doi/abs/10.1029/2020SW002497> doi:

- 671 10.1029/2020SW002497
- 672 Divett, T., Richardson, G. S., Beggan, C. D., Rodger, C. J., Boteler, D. H., Ingham,
673 M., ... Dalzell, M. (2018, jun). Transformer-Level Modeling of Geomagneti-
674 cally Induced Currents in New Zealand's South Island. *Space Weather*, *16*(6),
675 718–735. Retrieved from <http://doi.wiley.com/10.1029/2018SW001814>
676 doi: 10.1029/2018SW001814
- 677 Eastwood, J. P., Hapgood, M. A., Biffis, E., Benedetti, D., Bisi, M. M., Green, L.,
678 ... Burnett, C. (2018, dec). Quantifying the Economic Value of Space Weather
679 Forecasting for Power Grids: An Exploratory Study. *Space Weather*, *16*(12),
680 2052–2067. Retrieved from <http://doi.wiley.com/10.1029/2018SW002003>
681 doi: 10.1029/2018SW002003
- 682 Echer, E., & Gonzalez, W. D. (2004, may). Geoeffectiveness of interplanetary
683 shocks, magnetic clouds, sector boundary crossings and their combined occur-
684 rence. *Geophysical Research Letters*, *31*(9), n/a–n/a. Retrieved from [http://](http://doi.wiley.com/10.1029/2003GL019199)
685 doi.wiley.com/10.1029/2003GL019199 doi: 10.1029/2003GL019199
- 686 Engebretson, M. J., Pilipenko, V. A., Steinmetz, E. S., Moldwin, M. B., Con-
687 nors, M. G., Boteler, D. H., ... Russell, C. T. (2021, feb). Nighttime
688 magnetic perturbation events observed in Arctic Canada: 3. Occurrence
689 and amplitude as functions of magnetic latitude, local time, and magnetic
690 disturbance indices. *Space Weather*, e2020SW002526. Retrieved from
691 <https://onlinelibrary.wiley.com/doi/10.1029/2020SW002526> doi:
692 10.1029/2020SW002526
- 693 Fiori, R. A. D., Boteler, D. H., & Gillies, D. M. (2014, jan). Assessment of GIC risk
694 due to geomagnetic sudden commencements and identification of the current
695 systems responsible. *Space Weather*, *12*(1), 76–91. Retrieved from [http://](http://doi.wiley.com/10.1002/2013SW000967)
696 doi.wiley.com/10.1002/2013SW000967 doi: 10.1002/2013SW000967
- 697 Forsyth, C., Rae, I. J., Coxon, J. C., Freeman, M. P., Jackman, C. M., Gjerloev,
698 J., & Fazakerley, A. N. (2015, dec). A new technique for determining
699 Substorm Onsets and Phases from Indices of the Electrojet (SOPHIE).
700 *Journal of Geophysical Research: Space Physics*, *120*(12), 10,592–10,606.
701 Retrieved from <http://doi.wiley.com/10.1002/2015JA021343> doi:
702 10.1002/2015JA021343
- 703 Forsyth, C., Shortt, M., Coxon, J. C., Rae, I. J., Freeman, M. P., Kalmoni,
704 N. M. E., ... Burrell, A. G. (2018, apr). Seasonal and Temporal Varia-
705 tions of Field-Aligned Currents and Ground Magnetic Deflections During
706 Substorms. *Journal of Geophysical Research: Space Physics*, *123*(4), 2696–
707 2713. Retrieved from <http://doi.wiley.com/10.1002/2017JA025136> doi:
708 10.1002/2017JA025136
- 709 Freeman, M. P., & Farrugia, C. J. (1998). Magnetopause Motions in a Newton-
710 Busemann Approach. In *Polar cap boundary phenomena* (pp. 15–26). Dor-
711 drecht: Springer Netherlands. Retrieved from [http://link.springer.com/10](http://link.springer.com/10.1007/978-94-011-5214-3_2)
712 [.1007/978-94-011-5214-3_2](http://link.springer.com/10.1007/978-94-011-5214-3_2) doi: 10.1007/978-94-011-5214-3_2
- 713 Freeman, M. P., Forsyth, C., & Rae, I. J. (2019, may). The influence of
714 substorms on extreme rates of change of the surface horizontal mag-
715 netic field in the U.K. *Space Weather*, 2018SW002148. Retrieved from
716 <https://onlinelibrary.wiley.com/doi/abs/10.1029/2018SW002148> doi:
717 10.1029/2018SW002148
- 718 Freeman, M. P., Freeman, N. C., & Farrugia, C. J. (1995, sep). A linear perturba-
719 tion analysis of magnetopause motion in the Newton-Busemann limit. *Annales*
720 *Geophysicae*, *13*(9), 907–918. Retrieved from [https://angeo.copernicus](https://angeo.copernicus.org/articles/13/907/1995/)
721 [.org/articles/13/907/1995/](https://angeo.copernicus.org/articles/13/907/1995/) doi: 10.1007/s00585-995-0907-0
- 722 Freeman, M. P., & Morley, S. K. (2004, jun). A minimal substorm model that ex-
723 plains the observed statistical distribution of times between substorms. *Geo-*
724 *physical Research Letters*, *31*(12), n/a–n/a. Retrieved from [http://doi.wiley](http://doi.wiley.com/10.1029/2004GL019989)
725 [.com/10.1029/2004GL019989](http://doi.wiley.com/10.1029/2004GL019989) doi: 10.1029/2004GL019989

- 726 Gonzalez, W. D., Joselyn, J. A., Kamide, Y., Kroehl, H. W., Ros, G., Tsuru, B. T.,
727 & Vasyliunas, V. M. (1994). *What is a geomagnetic storm?* (Vol. 99; Tech.
728 Rep. No. A4). Retrieved from [https://agupubs.onlinelibrary.wiley.com/](https://agupubs.onlinelibrary.wiley.com/doi/pdf/10.1029/93JA02867)
729 [doi/pdf/10.1029/93JA02867](https://doi.org/10.1029/93JA02867) doi: 10.1029/93JA02867
- 730 Gosling, J. T., McComas, D. J., Phillips, J. L., & Bame, S. J. (1991, may). Geo-
731 magnetic activity associated with earth passage of interplanetary shock distur-
732 bances and coronal mass ejections. *Journal of Geophysical Research*, *96*(A5),
733 7831. Retrieved from <http://doi.wiley.com/10.1029/91JA00316> doi:
734 10.1029/91JA00316
- 735 Huang, C.-S., Le, G., & Reeves, G. D. (2004, jul). Periodic magnetospheric sub-
736 storms during fluctuating interplanetary magnetic field $\delta B_i / i_i$ $\delta z_i / i_i$
737 $\delta j / \delta j_i$. *Geophysical Research Letters*, *31*(14), L14801. Retrieved from [http://](http://doi.wiley.com/10.1029/2004GL020180)
738 doi.wiley.com/10.1029/2004GL020180 doi: 10.1029/2004GL020180
- 739 Hübner, J., Beggan, C. D., Richardson, G. S., Martyn, T., & Thomson, A. W. P.
740 (2020, apr). Differential Magnetometer Measurements of Geomagnetically
741 Induced Currents in a Complex High Voltage Network. *Space Weather*, *18*(4).
742 Retrieved from [https://onlinelibrary.wiley.com/doi/abs/10.1029/](https://onlinelibrary.wiley.com/doi/abs/10.1029/2019SW002421)
743 [2019SW002421](https://onlinelibrary.wiley.com/doi/abs/10.1029/2019SW002421) doi: 10.1029/2019SW002421
- 744 Hunter, J. D. (2007). Matplotlib: A 2D graphics environment. *Computing in Science*
745 *and Engineering*, *9*(3), 90–95. Retrieved from [http://ieeexplore.ieee.org/](http://ieeexplore.ieee.org/document/4160265/)
746 [document/4160265/](http://ieeexplore.ieee.org/document/4160265/) doi: 10.1109/MCSE.2007.55
- 747 Joselyn, J. A., & Tsurutani, B. T. (1990, nov). Geomagnetic Sudden im-
748 pulses and storm sudden commencements: A note on terminology. *Eos*,
749 *Transactions American Geophysical Union*, *71*(47), 1808. Retrieved from
750 <http://doi.wiley.com/10.1029/90EO00350> doi: 10.1029/90EO00350
- 751 Kappenman, J. G. (1996, may). Geomagnetic storms and their impact on power
752 systems. *IEEE Power Engineering Review*, *16*(5), 5. Retrieved from [http://](http://ieeexplore.ieee.org/document/491910/)
753 ieeexplore.ieee.org/document/491910/ doi: 10.1109/MPER.1996.491910
- 754 Kappenman, J. G. (2003, dec). Storm sudden commencement events and the
755 associated geomagnetically induced current risks to ground-based systems
756 at low-latitude and midlatitude locations. *Space Weather*, *1*(3), n/a–n/a.
757 Retrieved from <http://doi.wiley.com/10.1029/2003SW000009> doi:
758 10.1029/2003SW000009
- 759 Kappenman, J. G., & Albertson, D. (1990, mar). Bracing for the geomag-
760 netic storms. *IEEE Spectrum*, *27*(3), 27–33. Retrieved from [http://](http://ieeexplore.ieee.org/document/48847/)
761 ieeexplore.ieee.org/document/48847/ doi: 10.1109/6.48847
- 762 Kilpua, E., Lugaz, N., Mays, M. L., & Temmer, M. (2019, apr). Forecasting the
763 Structure and Orientation of Earthbound Coronal Mass Ejections. *Space*
764 *Weather*, *17*(4), 498–526. Retrieved from [https://onlinelibrary.wiley](https://onlinelibrary.wiley.com/doi/abs/10.1029/2018SW001944)
765 [.com/doi/abs/10.1029/2018SW001944](https://onlinelibrary.wiley.com/doi/abs/10.1029/2018SW001944) doi: 10.1029/2018SW001944
- 766 Kokubun, S., McPherron, R. L., & Russell, C. T. (1977, jan). Triggering of sub-
767 storms by solar wind discontinuities. *Journal of Geophysical Research*, *82*(1),
768 74–86. Retrieved from <http://doi.wiley.com/10.1029/JA082i001p00074>
769 doi: 10.1029/JA082i001p00074
- 770 Lee, D.-Y., Lyons, L. R., Kim, K. C., Baek, J.-H., Kim, K.-H., Kim, H.-J., ... Han,
771 W. (2006, dec). Repetitive substorms caused by Alfvénic waves of the in-
772 terplanetary magnetic field during high-speed solar wind streams. *Jour-*
773 *nal of Geophysical Research*, *111*(A12), A12214. Retrieved from [http://](http://doi.wiley.com/10.1029/2006JA011685)
774 doi.wiley.com/10.1029/2006JA011685 doi: 10.1029/2006JA011685
- 775 Lühr, H., Schlegel, K., Araki, T., Rother, M., & Förster, M. (2009, may). Night-time
776 sudden commencements observed by CHAMP and ground-based magnetome-
777 ters and their relationship to solar wind parameters. *Annales Geophysicae*,
778 *27*(5), 1897–1907. Retrieved from [https://www.ann-geophys.net/27/1897/](https://www.ann-geophys.net/27/1897/2009/)
779 [2009/](https://www.ann-geophys.net/27/1897/2009/) doi: 10.5194/angeo-27-1897-2009
- 780 Mac Manus, D. H., Rodger, C. J., Dalzell, M., Thomson, A. W. P., Clilverd,

- 781 M. A., Petersen, T., ... Divett, T. (2017, aug). Long-term geomagnet-
 782 ically induced current observations in New Zealand: Earth return correc-
 783 tions and geomagnetic field driver. *Space Weather*, 15(8), 1020–1038.
 784 Retrieved from <http://doi.wiley.com/10.1002/2017SW001635> doi:
 785 10.1002/2017SW001635
- 786 Maimaiti, M., Kunduri, B., Ruohoniemi, J. M., Baker, J. B. H., & House, L. L.
 787 (2019, sep). A deep learning based approach to forecast the onset of
 788 magnetic substorms. *Space Weather*, 2019SW002251. Retrieved from
 789 <https://onlinelibrary.wiley.com/doi/abs/10.1029/2019SW002251> doi:
 790 10.1029/2019SW002251
- 791 Marshall, R. A., Dalzell, M., Waters, C. L., Goldthorpe, P., & Smith, E. A. (2012,
 792 aug). Geomagnetically induced currents in the New Zealand power network.
 793 *Space Weather*, 10(8), n/a–n/a. Retrieved from [http://doi.wiley.com/10](http://doi.wiley.com/10.1029/2012SW000806)
 794 [.1029/2012SW000806](http://doi.wiley.com/10.1029/2012SW000806) doi: 10.1029/2012SW000806
- 795 Mayaud, P. N. (1973). A hundred year series of geomagnetic data, 1868-1967: in-
 796 dices aa, storm sudden commencements(SSC). *IUGG Publ. Office*, 256.
- 797 McKinney, W. (2010). *Data Structures for Statistical Computing in Python*. Re-
 798 trieved from [http://conference.scipy.org/proceedings/scipy2010/](http://conference.scipy.org/proceedings/scipy2010/mckinney.html)
 799 [mckinney.html](http://conference.scipy.org/proceedings/scipy2010/mckinney.html)
- 800 McPherron, R. L., Aubry, . M. P., Russell, C. T., & Coleman, P. J. (1973).
 801 *Satellite Studies of Magnetospheric Substorms on August 15, 1968 4. Ogo 5*
 802 *Magnetic Field Observations* (Vol. 78; Tech. Rep. No. 16). Retrieved from
 803 [https://www.researchgate.net/profile/Robert_Mcpherron/publication/](https://www.researchgate.net/profile/Robert_Mcpherron/publication/254933902_Satellite_Studies_of_Magnetospheric_Substorms_on_August_15_1968/links/5adf4d5aa6fdcc29358e13ed/Satellite-Studies-of-Magnetospheric-Substorms-on-August-15-1968.pdf)
 804 [254933902_Satellite_Studies_of_Magnetospheric_Substorms_on_August](https://www.researchgate.net/profile/Robert_Mcpherron/publication/254933902_Satellite_Studies_of_Magnetospheric_Substorms_on_August_15_1968/links/5adf4d5aa6fdcc29358e13ed/Satellite-Studies-of-Magnetospheric-Substorms-on-August-15-1968.pdf)
 805 [_15_1968/links/5adf4d5aa6fdcc29358e13ed/Satellite-Studies-of](https://www.researchgate.net/profile/Robert_Mcpherron/publication/254933902_Satellite_Studies_of_Magnetospheric_Substorms_on_August_15_1968/links/5adf4d5aa6fdcc29358e13ed/Satellite-Studies-of-Magnetospheric-Substorms-on-August-15-1968.pdf)
 806 [-Magnetospheric-Substorms-on-August-15-1968.pdf](https://www.researchgate.net/profile/Robert_Mcpherron/publication/254933902_Satellite_Studies_of_Magnetospheric_Substorms_on_August_15_1968/links/5adf4d5aa6fdcc29358e13ed/Satellite-Studies-of-Magnetospheric-Substorms-on-August-15-1968.pdf)
- 807 Morley, S., Rouillard, A., & Freeman, M. (2009, jul). Recurrent substorm ac-
 808 tivity during the passage of a corotating interaction region. *Journal of*
 809 *Atmospheric and Solar-Terrestrial Physics*, 71(10-11), 1073–1081. Re-
 810 trieved from [https://www.sciencedirect.com/science/article/abs/](https://www.sciencedirect.com/science/article/abs/pii/S1364682608003611?via%3Dihub)
 811 [pii/S1364682608003611?via%3Dihub](https://www.sciencedirect.com/science/article/abs/pii/S1364682608003611?via%3Dihub) doi: 10.1016/J.JASTP.2008.11.009
- 812 Morley, S. K., & Freeman, M. P. (2007, apr). On the association between northward
 813 turnings of the interplanetary magnetic field and substorm onsets. *Geophys-
 814 ical Research Letters*, 34(8). Retrieved from [http://doi.wiley.com/10.1029/](http://doi.wiley.com/10.1029/2006GL028891)
 815 [2006GL028891](http://doi.wiley.com/10.1029/2006GL028891) doi: 10.1029/2006GL028891
- 816 Ngwira, C. M., Pulkkinen, A., Leila Mays, M., Kuznetsova, M. M., Galvin, A. B.,
 817 Simunac, K., ... Glocer, A. (2013, dec). Simulation of the 23 July 2012
 818 extreme space weather event: What if this extremely rare CME was Earth
 819 directed? *Space Weather*, 11(12), 671–679. Retrieved from [http://](http://doi.wiley.com/10.1002/2013SW000990)
 820 doi.wiley.com/10.1002/2013SW000990 doi: 10.1002/2013SW000990
- 821 Ngwira, C. M., Pulkkinen, A., Wilder, F. D., & Crowley, G. (2013, mar). Ex-
 822 tended study of extreme geoelectric field event scenarios for geomagnetically
 823 induced current applications. *Space Weather*, 11(3), 121–131. Retrieved from
 824 <http://doi.wiley.com/10.1002/swe.20021> doi: 10.1002/swe.20021
- 825 Ngwira, C. M., Pulkkinen, A. A., Bernabeu, E., Eichner, J., Viljanen, A., &
 826 Crowley, G. (2015, sep). Characteristics of extreme geoelectric fields
 827 and their possible causes: Localized peak enhancements. *Geophysical Re-
 828 search Letters*, 42(17), 6916–6921. Retrieved from [https://agupubs](https://agupubs.onlinelibrary.wiley.com/doi/full/10.1002/2015GL065061%4010.1002/%28ISSN%291542-7390.GIC15)
 829 [.onlinelibrary.wiley.com/doi/full/10.1002/2015GL065061%4010.1002/](https://agupubs.onlinelibrary.wiley.com/doi/full/10.1002/2015GL065061%4010.1002/%28ISSN%291542-7390.GIC15)
 830 [%28ISSN%291542-7390.GIC15](https://agupubs.onlinelibrary.wiley.com/doi/full/10.1002/2015GL065061%4010.1002/%28ISSN%291542-7390.GIC15) doi: 10.1002/2015GL065061
- 831 Odstrcil, D. (2003, aug). Modeling 3-D solar wind structure. *Advances in Space*
 832 *Research*, 32(4), 497–506. Retrieved from [https://www.sciencedirect.com/](https://www.sciencedirect.com/science/article/abs/pii/S0273117703003326?via%3Dihub)
 833 [science/article/abs/pii/S0273117703003326?via%3Dihub](https://www.sciencedirect.com/science/article/abs/pii/S0273117703003326?via%3Dihub) doi: 10.1016/
 834 [S0273-1177\(03\)00332-6](https://www.sciencedirect.com/science/article/abs/pii/S0273117703003326?via%3Dihub)
- 835 Oliveira, D., & Samsonov, A. (2018, jan). Geoeffectiveness of interplanetary shocks

- 836 controlled by impact angles: A review. *Advances in Space Research*, 61(1), 1–
 837 44. Retrieved from [https://www.sciencedirect.com/science/article/pii/](https://www.sciencedirect.com/science/article/pii/S0273117717307275?via%3Dihub)
 838 [S0273117717307275?via%3Dihub](https://www.sciencedirect.com/science/article/pii/S0273117717307275?via%3Dihub) doi: 10.1016/J.ASR.2017.10.006
- 839 Oliveira, D. M., Arel, D., Raeder, J., Zesta, E., Ngwira, C. M., Carter, B. A., ...
 840 Gjerloev, J. W. (2018, jun). Geomagnetically Induced Currents Caused
 841 by Interplanetary Shocks With Different Impact Angles and Speeds. *Space*
 842 *Weather*, 16(6), 636–647. Retrieved from [http://doi.wiley.com/10.1029/](http://doi.wiley.com/10.1029/2018SW001880)
 843 [2018SW001880](http://doi.wiley.com/10.1029/2018SW001880) doi: 10.1029/2018SW001880
- 844 Oughton, E. J., Hapgood, M., Richardson, G. S., Beggan, C. D., Thomson,
 845 A. W. P., Gibbs, M., ... Horne, R. B. (2019, may). A Risk Assess-
 846 ment Framework for the Socioeconomic Impacts of Electricity Transmis-
 847 sion Infrastructure Failure Due to Space Weather: An Application to the
 848 United Kingdom. *Risk Analysis*, 39(5), 1022–1043. Retrieved from
 849 <https://onlinelibrary.wiley.com/doi/abs/10.1111/risa.13229> doi:
 850 [10.1111/risa.13229](https://onlinelibrary.wiley.com/doi/abs/10.1111/risa.13229)
- 851 Oughton, E. J., Skelton, A., Horne, R. B., Thomson, A. W. P., & Gaunt, C. T.
 852 (2017, jan). Quantifying the daily economic impact of extreme space weather
 853 due to failure in electricity transmission infrastructure. *Space Weather*, 15(1),
 854 65–83. Retrieved from <http://doi.wiley.com/10.1002/2016SW001491> doi:
 855 [10.1002/2016SW001491](http://doi.wiley.com/10.1002/2016SW001491)
- 856 Owens, M., Lang, M., Barnard, L., Riley, P., Ben-Nun, M., Scott, C. J., ... Gonzi,
 857 S. (2020, mar). A Computationally Efficient, Time-Dependent Model of
 858 the Solar Wind for Use as a Surrogate to Three-Dimensional Numerical
 859 Magnetohydrodynamic Simulations. *Solar Physics*, 295(3), 43. Retrieved
 860 from <http://link.springer.com/10.1007/s11207-020-01605-3> doi:
 861 [10.1007/s11207-020-01605-3](http://link.springer.com/10.1007/s11207-020-01605-3)
- 862 Owens, M. J., & Riley, P. (2017, nov). Probabilistic Solar Wind Forecast-
 863 ing Using Large Ensembles of Near-Sun Conditions With a Simple One-
 864 Dimensional “Upwind” Scheme. *Space Weather*, 15(11), 1461–1474.
 865 Retrieved from <http://doi.wiley.com/10.1002/2017SW001679> doi:
 866 [10.1002/2017SW001679](http://doi.wiley.com/10.1002/2017SW001679)
- 867 Oyedokun, D., Heyns, M., Cilliers, P., & Gaunt, C. (2020, jan). Frequency Com-
 868 ponents of Geomagnetically Induced Currents for Power System Modelling.
 869 In *2020 international sauppec/robmech/prasa conference* (pp. 1–6). IEEE.
 870 Retrieved from <https://ieeexplore.ieee.org/document/9041021/> doi:
 871 [10.1109/SAUPEC/RobMech/PRASA48453.2020.9041021](https://ieeexplore.ieee.org/document/9041021/)
- 872 Pedregosa, F., Varoquaux, G., Gramfort, A., Michel, V., Thirion, B., Grisel, O., ...
 873 Duchesnay, É. (2011). Scikit-learn: Machine Learning in Python. *Jour-
 874 nal of Machine Learning Research*, 12(Oct), 2825–2830. Retrieved from
 875 <http://jmlr.org/papers/v12/pedregosa11a.html>
- 876 Pulkkinen, A., Lindahl, S., Viljanen, A., & Pirjola, R. (2005, aug). Geomagnetic
 877 storm of 29–31 October 2003: Geomagnetically induced currents and their rela-
 878 tion to problems in the Swedish high-voltage power transmission system. *Space*
 879 *Weather*, 3(8), n/a–n/a. Retrieved from [http://doi.wiley.com/10.1029/](http://doi.wiley.com/10.1029/2004SW000123)
 880 [2004SW000123](http://doi.wiley.com/10.1029/2004SW000123) doi: 10.1029/2004SW000123
- 881 Richardson, I. G., & Cane, H. V. (2012, may). Near-earth solar wind flows and
 882 related geomagnetic activity during more than four solar cycles (1963–2011).
 883 *Journal of Space Weather and Space Climate*, 2, A02. Retrieved from [http://](http://www.swsc-journal.org/10.1051/swsc/2012003)
 884 www.swsc-journal.org/10.1051/swsc/2012003 doi: 10.1051/swsc/2012003
- 885 Rodger, C. J., Mac Manus, D. H., Dalzell, M., Thomson, A. W. P., Clarke, E.,
 886 Petersen, T., ... Divett, T. (2017, nov). Long-Term Geomagnetically In-
 887 duced Current Observations From New Zealand: Peak Current Estimates
 888 for Extreme Geomagnetic Storms. *Space Weather*, 15(11), 1447–1460.
 889 Retrieved from <http://doi.wiley.com/10.1002/2017SW001691> doi:
 890 [10.1002/2017SW001691](http://doi.wiley.com/10.1002/2017SW001691)

- 891 Rogers, N. C., Wild, J. A., Eastoe, E. F., Gjerloev, J. W., & Thomson, A. W. P.
892 (2020, feb). A global climatological model of extreme geomagnetic field
893 fluctuations. *Journal of Space Weather and Space Climate*, 10, 5. Re-
894 trieved from <https://www.swsc-journal.org/10.1051/swsc/2020008> doi:
895 10.1051/swsc/2020008
- 896 Shore, R. M., Freeman, M. P., Coxon, J. C., Thomas, E. G., Gjerloev, J. W.,
897 & Olsen, N. (2019, jul). Spatial Variation in the Responses of the Sur-
898 face External and Induced Magnetic Field to the Solar Wind. *Journal of*
899 *Geophysical Research: Space Physics*, 124(7), 6195–6211. Retrieved from
900 <https://onlinelibrary.wiley.com/doi/10.1029/2019JA026543> doi:
901 10.1029/2019JA026543
- 902 Smith, A. W., Freeman, M. P., Rae, I. J., & Forsyth, C. (2019, nov). The Influence
903 of Sudden Commencements on the Rate of Change of the Surface Horizon-
904 tal Magnetic Field in the United Kingdom. *Space Weather*, 2019SW002281.
905 Retrieved from [https://onlinelibrary.wiley.com/doi/abs/10.1029/](https://onlinelibrary.wiley.com/doi/abs/10.1029/2019SW002281)
906 [2019SW002281](https://onlinelibrary.wiley.com/doi/abs/10.1029/2019SW002281) doi: 10.1029/2019SW002281
- 907 Smith, A. W., Rae, I. J., Forsyth, C., Oliveira, D. M., Freeman, M. P., & Jackson,
908 D. R. (2020, nov). Probabilistic Forecasts of Storm Sudden Commence-
909 ments From Interplanetary Shocks Using Machine Learning. *Space Weather*,
910 18(11). Retrieved from [https://onlinelibrary.wiley.com/doi/10.1029/](https://onlinelibrary.wiley.com/doi/10.1029/2020SW002603)
911 [2020SW002603](https://onlinelibrary.wiley.com/doi/10.1029/2020SW002603) doi: 10.1029/2020SW002603
- 912 Takeuchi, T., Araki, T., Viljanen, A., & Watermann, J. (2002, jul). Geomagnetic
913 negative sudden impulses: Interplanetary causes and polarization distribution.
914 *Journal of Geophysical Research*, 107(A7), 1096. Retrieved from [http://](http://doi.wiley.com/10.1029/2001JA900152)
915 doi.wiley.com/10.1029/2001JA900152 doi: 10.1029/2001JA900152
- 916 Tanskanen, E., Pulkkinen, T. I., Koskinen, H. E. J., & Slavin, J. A. (2002,
917 jun). Substorm energy budget during low and high solar activity: 1997
918 and 1999 compared. *Journal of Geophysical Research*, 107(A6), 1086.
919 Retrieved from <http://doi.wiley.com/10.1029/2001JA900153> doi:
920 10.1029/2001JA900153
- 921 Thomson, A. W., Dawson, E. B., & Reay, S. J. (2011, oct). Quantifying extreme be-
922 havior in geomagnetic activity. *Space Weather*, 9(10). Retrieved from [http://](http://doi.wiley.com/10.1029/2011SW000696)
923 doi.wiley.com/10.1029/2011SW000696 doi: 10.1029/2011SW000696
- 924 Thomson, A. W., McKay, A. J., Clarke, E., & Reay, S. J. (2005, nov). Surface
925 electric fields and geomagnetically induced currents in the Scottish Power grid
926 during the 30 October 2003 geomagnetic storm. *Space Weather*, 3(11), n/a–
927 n/a. Retrieved from <http://doi.wiley.com/10.1029/2005SW000156> doi:
928 10.1029/2005sw000156
- 929 Turnbull, K. L., Wild, J. A., Honary, F., Thomson, A. W. P., & McKay, A. J. (2009,
930 sep). Characteristics of variations in the ground magnetic field during sub-
931 storms at mid latitudes. *Annales Geophysicae*, 27(9), 3421–3428. Retrieved
932 from <https://angeo.copernicus.org/articles/27/3421/2009/> doi:
933 10.5194/angeo-27-3421-2009
- 934 Turner, D. L., O’Brien, T. P., Fennell, J. F., Claudepierre, S. G., Blake, J. B.,
935 Kilpua, E. K. J., & Hietala, H. (2015, nov). The effects of geomagnetic storms
936 on electrons in Earth’s radiation belts. *Geophysical Research Letters*, 42(21),
937 9176–9184. Retrieved from <http://doi.wiley.com/10.1002/2015GL064747>
938 doi: 10.1002/2015GL064747
- 939 Van Der Walt, S., Colbert, S. C., & Varoquaux, G. (2011, mar). The NumPy array:
940 A structure for efficient numerical computation. *Computing in Science and*
941 *Engineering*, 13(2), 22–30. Retrieved from [http://ieeexplore.ieee.org/](http://ieeexplore.ieee.org/document/5725236/)
942 [document/5725236/](http://ieeexplore.ieee.org/document/5725236/) doi: 10.1109/MCSE.2011.37
- 943 Viljanen, A., Amm, O., & Pirjola, R. (1999, dec). Modeling geomagnetically in-
944 duced currents during different ionospheric situations. *Journal of Geophysical*
945 *Research: Space Physics*, 104(A12), 28059–28071. Retrieved from <http://doi>

- 946 .wiley.com/10.1029/1999JA900337 doi: 10.1029/1999JA900337
 947 Viljanen, A., Nevanlinna, H., Pajunpää, K., & Pulkkinen, A. (2001). Time deriva-
 948 tive of the horizontal geomagnetic field as an activity indicator. *Annales Geo-*
 949 *physicae*, 19(9), 1107–1118. Retrieved from [http://www.ann-geophys.net/](http://www.ann-geophys.net/19/1107/2001/)
 950 [19/1107/2001/](http://www.ann-geophys.net/19/1107/2001/) doi: 10.5194/angeo-19-1107-2001
- 951 Viljanen, A., & Pirjola, R. (1994, jul). Geomagnetically induced currents in the
 952 Finnish high-voltage power system. *Surveys in Geophysics*, 15(4), 383–408.
 953 Retrieved from <http://link.springer.com/10.1007/BF00665999> doi:
 954 10.1007/BF00665999
- 955 Viljanen, A., Pirjola, R., Prácsér, E., Ahmadzai, S., & Singh, V. (2013). Geo-
 956 magnetically induced currents in Europe: Characteristics based on a lo-
 957 cal power grid model. *Space Weather*, 11(10), 575–584. Retrieved from
 958 <http://real.mtak.hu/2957/> doi: 10.1002/swe.20098
- 959 Viljanen, A., Tanskanen, E. I., & Pulkkinen, A. (2006, mar). Relation be-
 960 tween substorm characteristics and rapid temporal variations of the ground
 961 magnetic field. *Annales Geophysicae*, 24(2), 725–733. Retrieved from
 962 <https://angeo.copernicus.org/articles/24/725/2006/> doi: 10.5194/
 963 angeo-24-725-2006
- 964 Virtanen, P., Gommers, R., Oliphant, T. E., Haberland, M., Reddy, T., Courn-
 965 peau, D., ... Contributors, S. . . (2020). SciPy 1.0: Fundamental Algorithms
 966 for Scientific Computing in Python. *Nature Methods*, 17, 261–272. doi:
 967 <https://doi.org/10.1038/s41592-019-0686-2>
- 968 Wang, C., Li, C. X., Huang, Z. H., & Richardson, J. D. (2006, jul). Effect
 969 of interplanetary shock strengths and orientations on storm sudden com-
 970 mencement rise times. *Geophysical Research Letters*, 33(14), L14104.
 971 Retrieved from <http://doi.wiley.com/10.1029/2006GL025966> doi:
 972 10.1029/2006GL025966
- 973 Yue, C., Zong, Q. G., Zhang, H., Wang, Y. F., Yuan, C. J., Pu, Z. Y., ... Wang,
 974 C. R. (2010, may). Geomagnetic activity triggered by interplanetary
 975 shocks. *Journal of Geophysical Research: Space Physics*, 115(A5), n/a–
 976 n/a. Retrieved from <http://doi.wiley.com/10.1029/2010JA015356> doi:
 977 10.1029/2010JA015356
- 978 Zhang, J. J., Wang, C., Sun, T. R., Liu, C. M., & Wang, K. R. (2015, oct). GIC
 979 due to storm sudden commencement in low-latitude high-voltage power net-
 980 work in China: Observation and simulation. *Space Weather*, 13(10), 643–
 981 655. Retrieved from <http://doi.wiley.com/10.1002/2015SW001263> doi:
 982 10.1002/2015SW001263
- 983 Zhou, X., & Tsurutani, B. T. (2001, sep). Interplanetary shock triggering of
 984 nightside geomagnetic activity: Substorms, pseudobreakups, and quiescent
 985 events. *Journal of Geophysical Research: Space Physics*, 106(A9), 18957–
 986 18967. Retrieved from <http://doi.wiley.com/10.1029/2000JA003028> doi:
 987 10.1029/2000JA003028

Figure 1.

-18 -12 -6 0 6 12 18 24



-18 -12 -6 0 6 12 18 24

Figure 2.

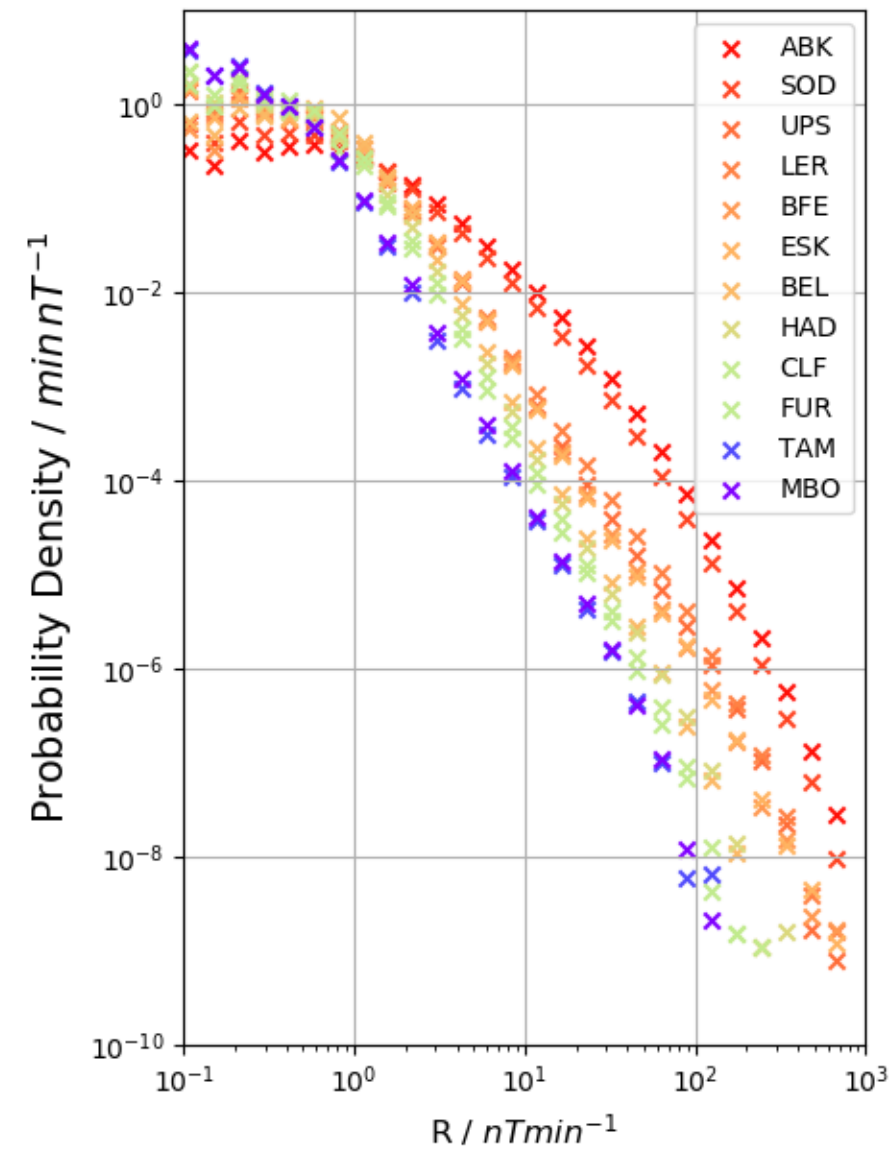
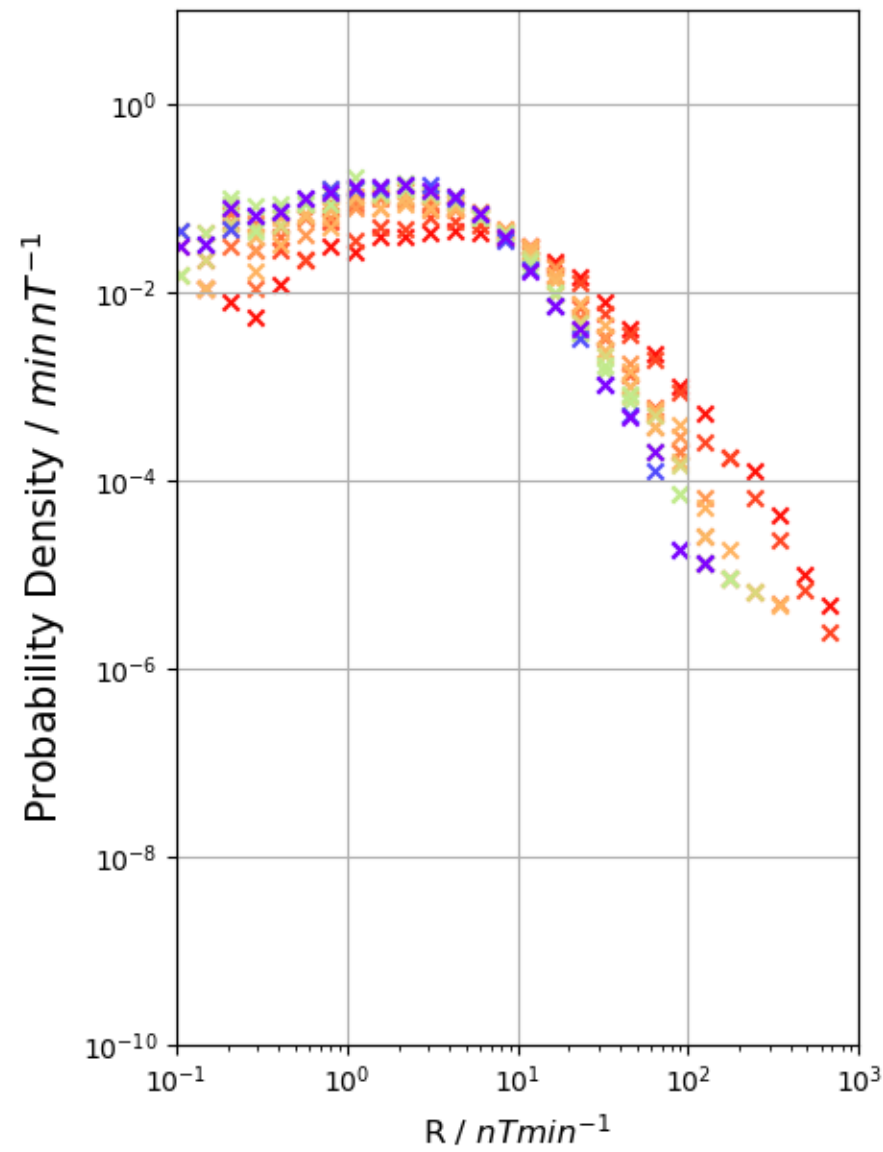
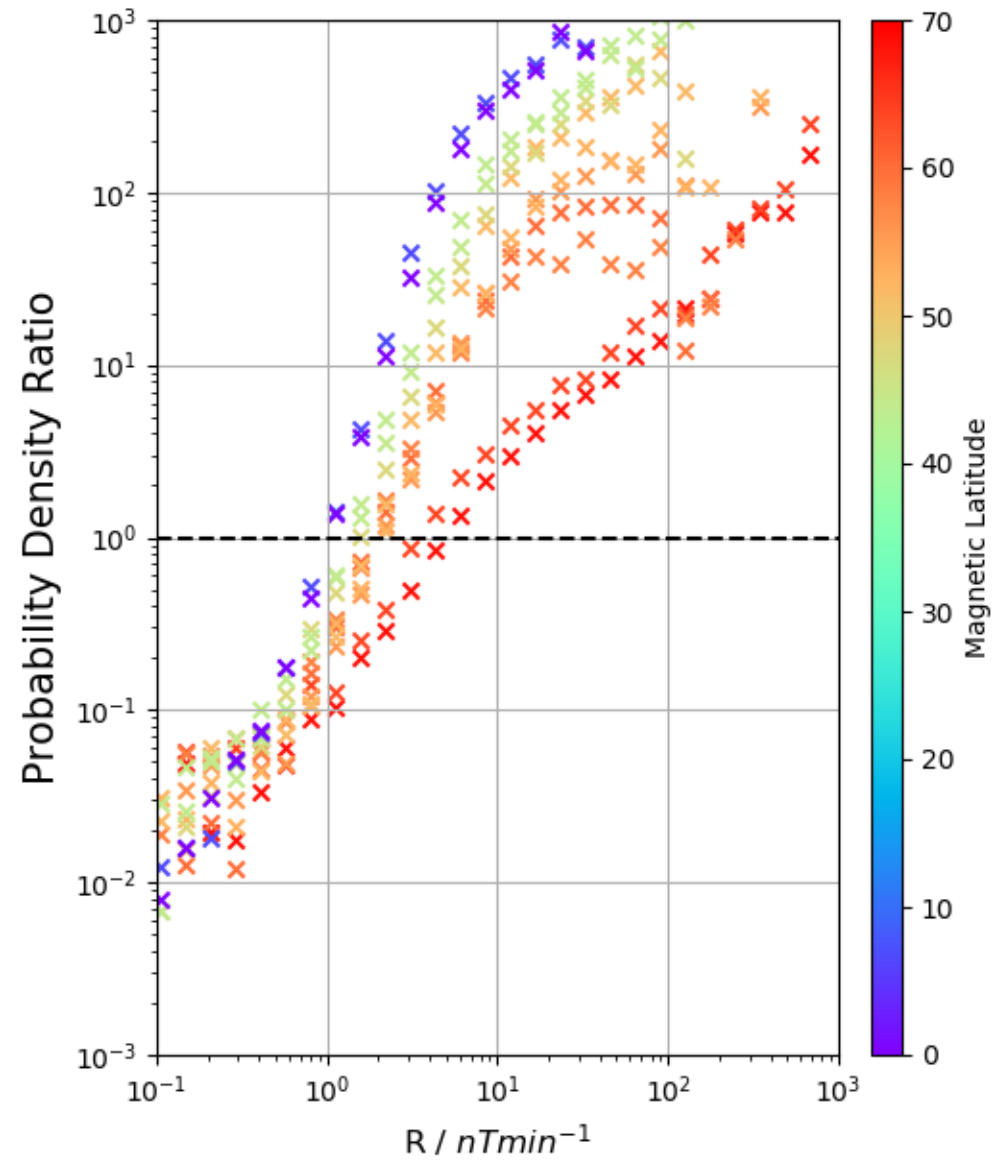
a All Data**b During SCs****c Ratio**

Figure 3.

All SCs

SSCs

SIs

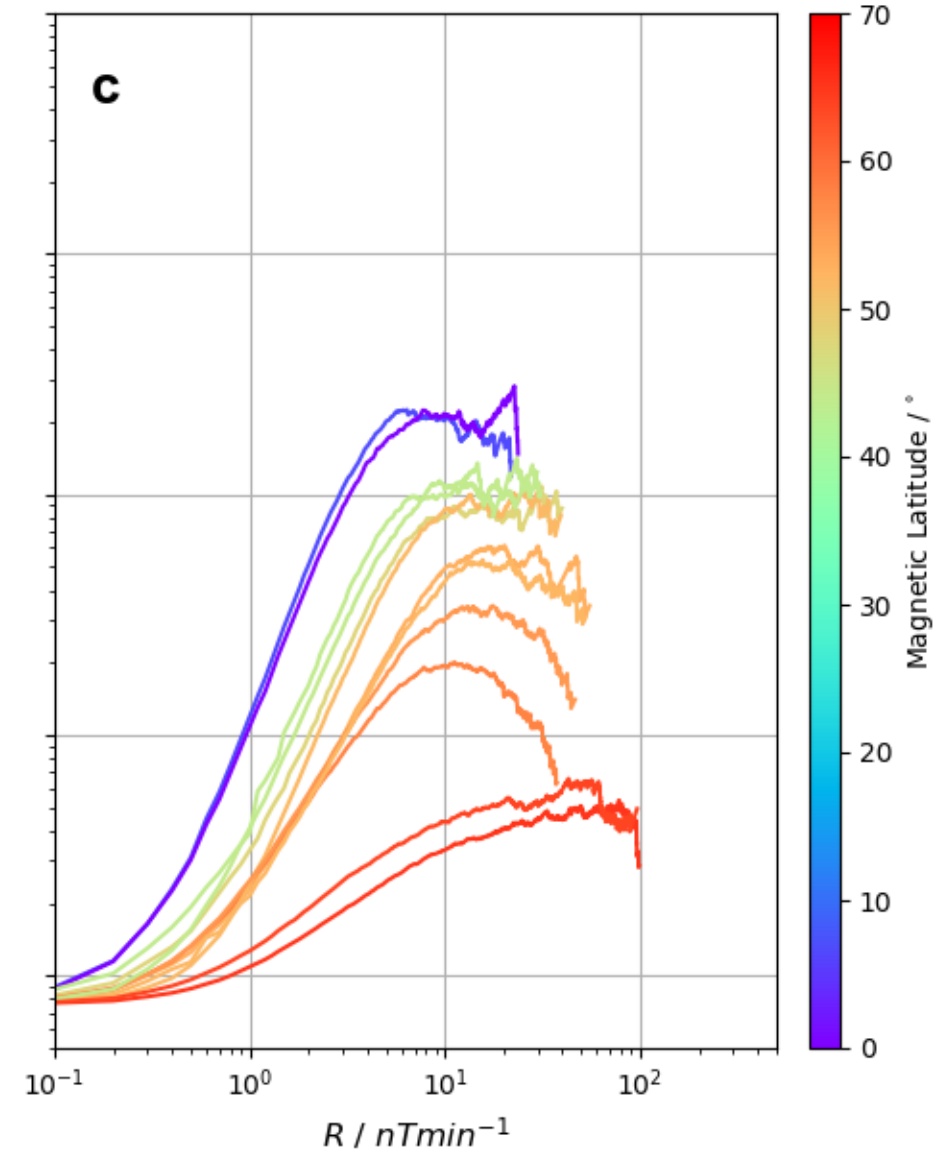
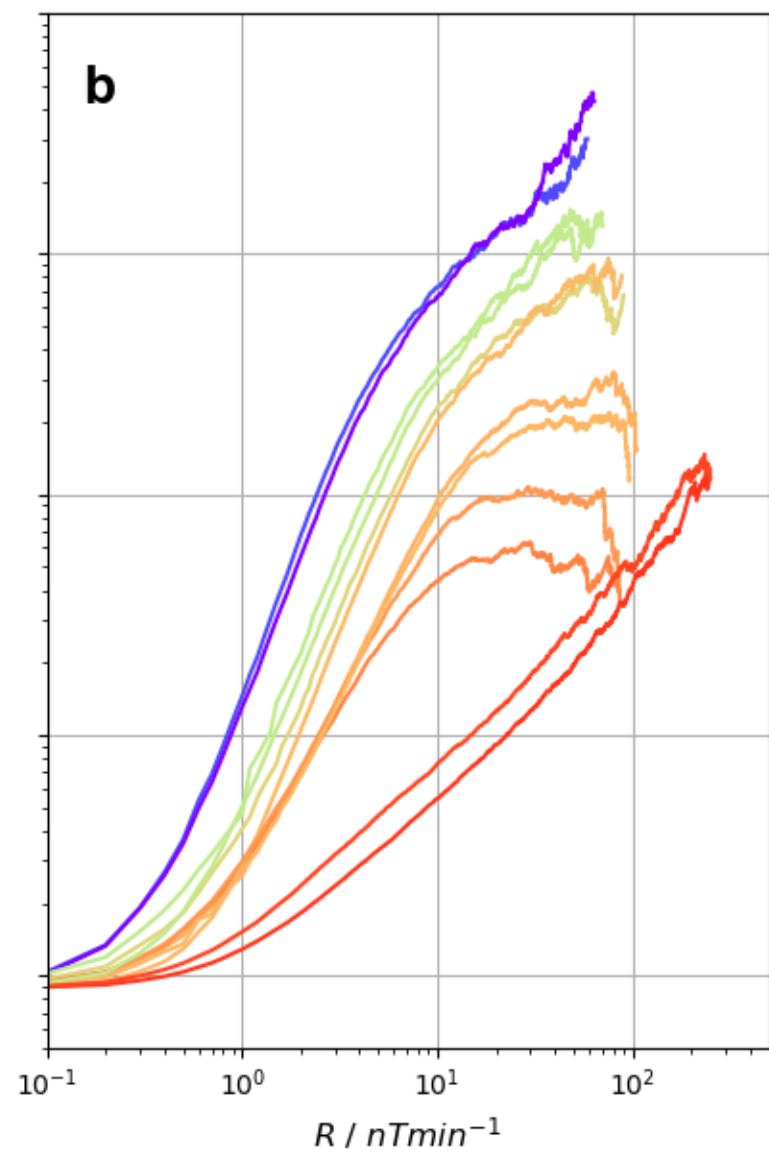
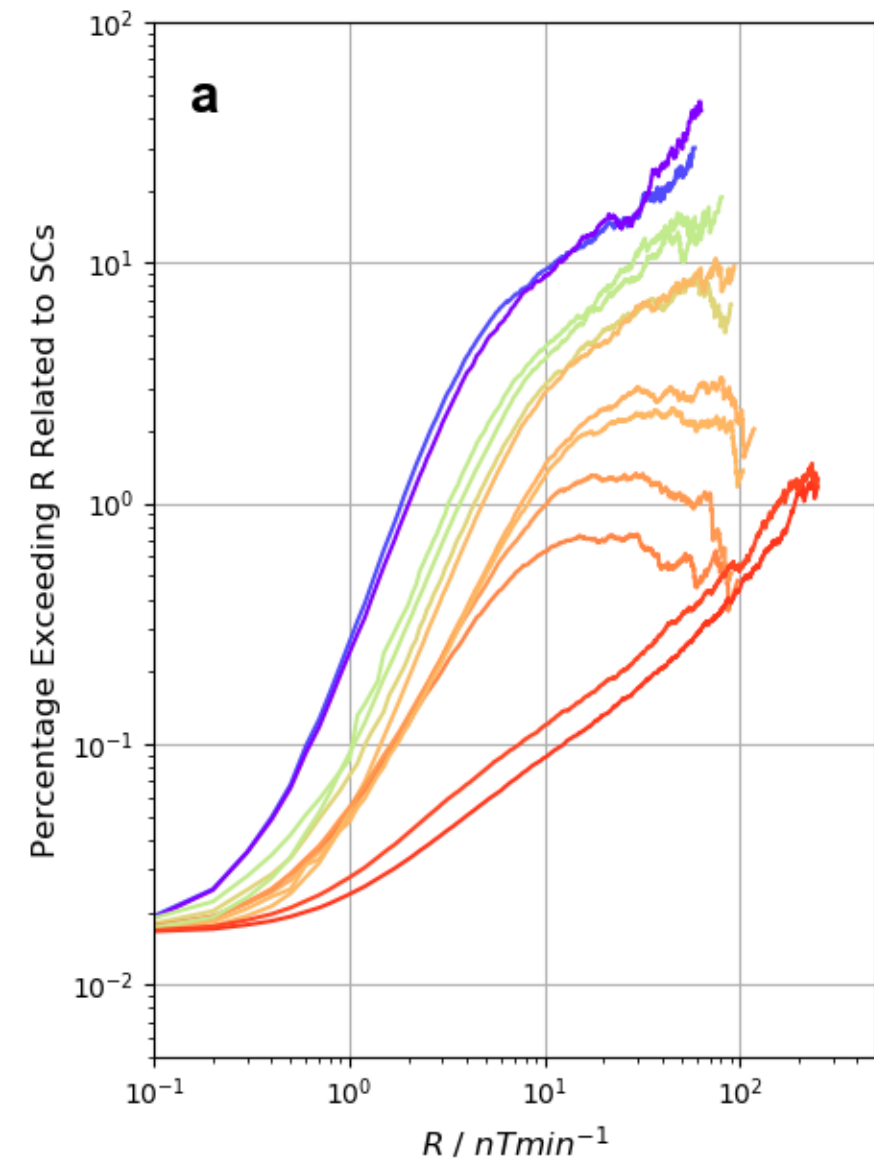


Figure 4.

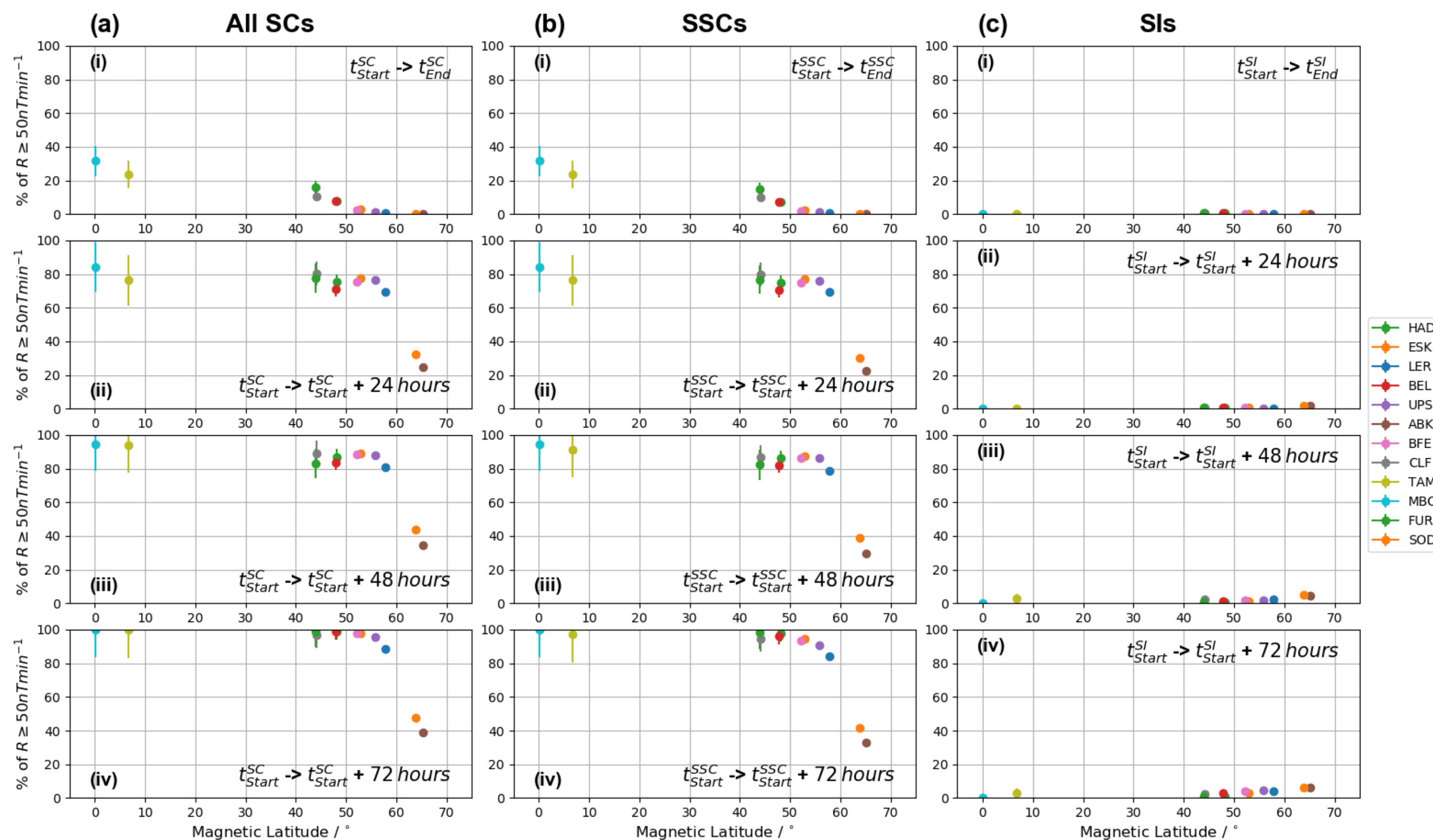


Figure 5.

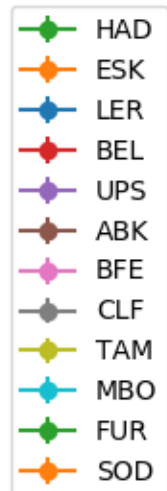
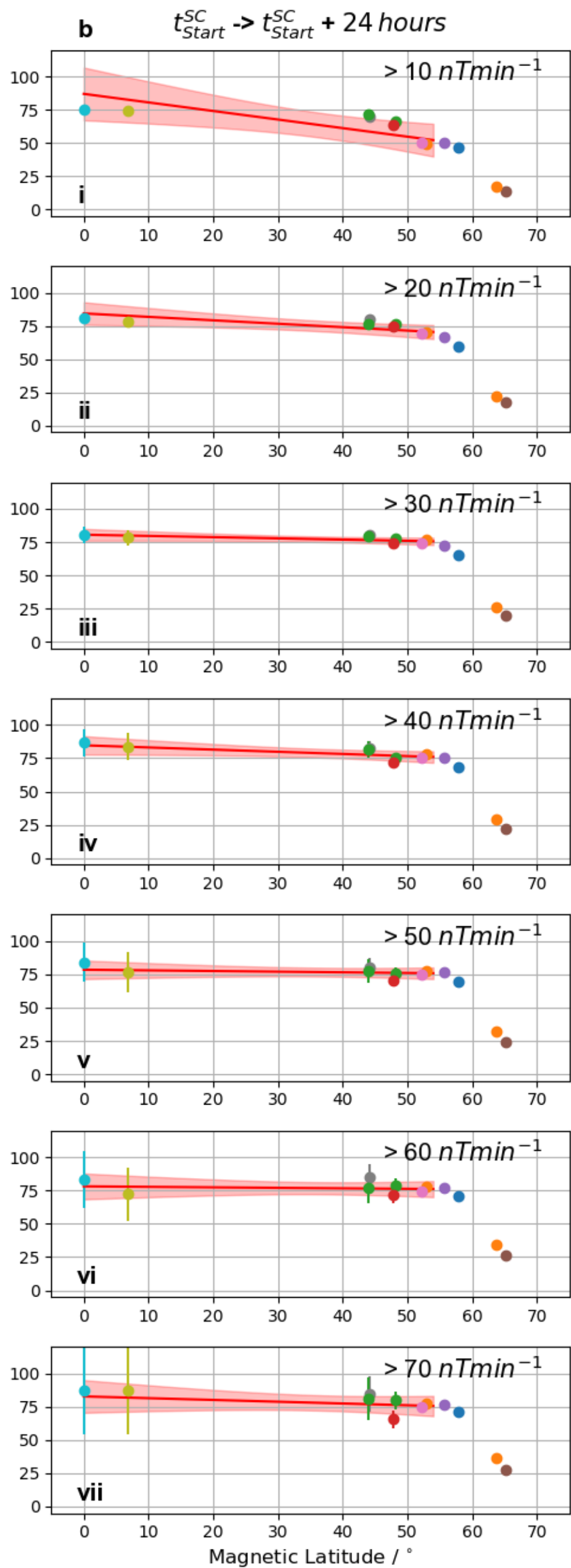
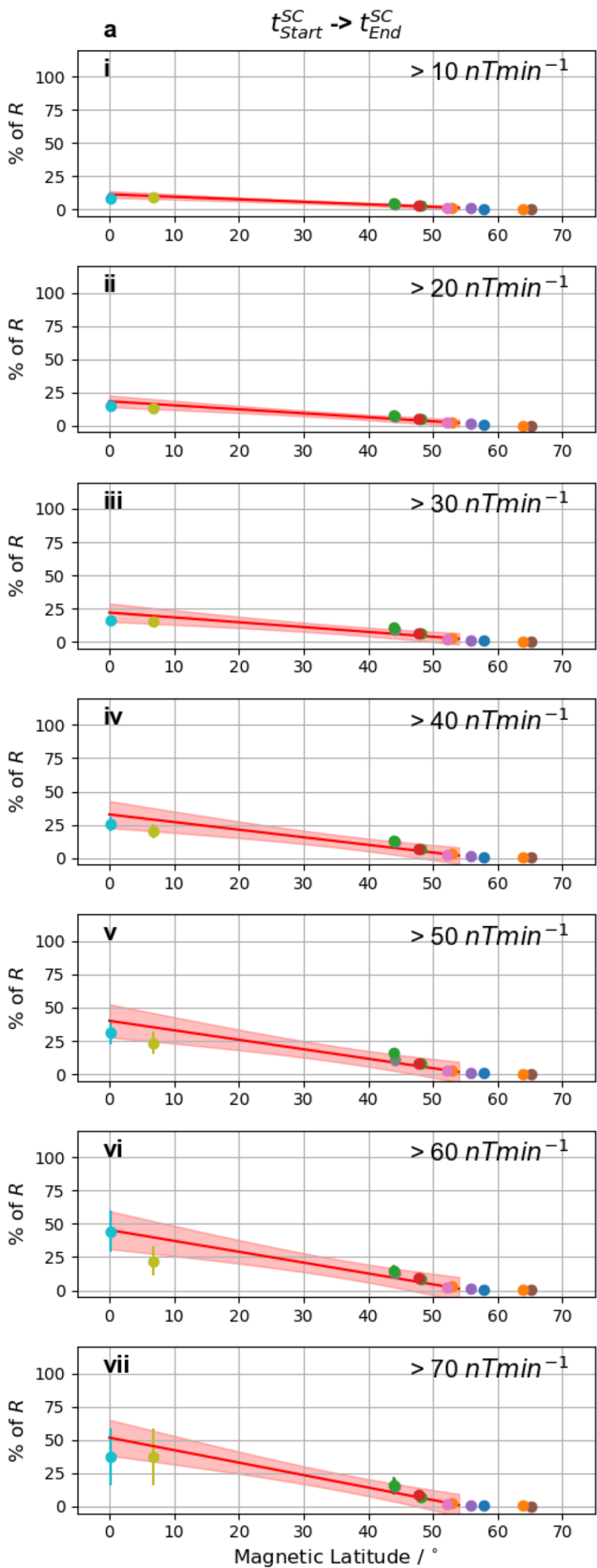


Figure 6.

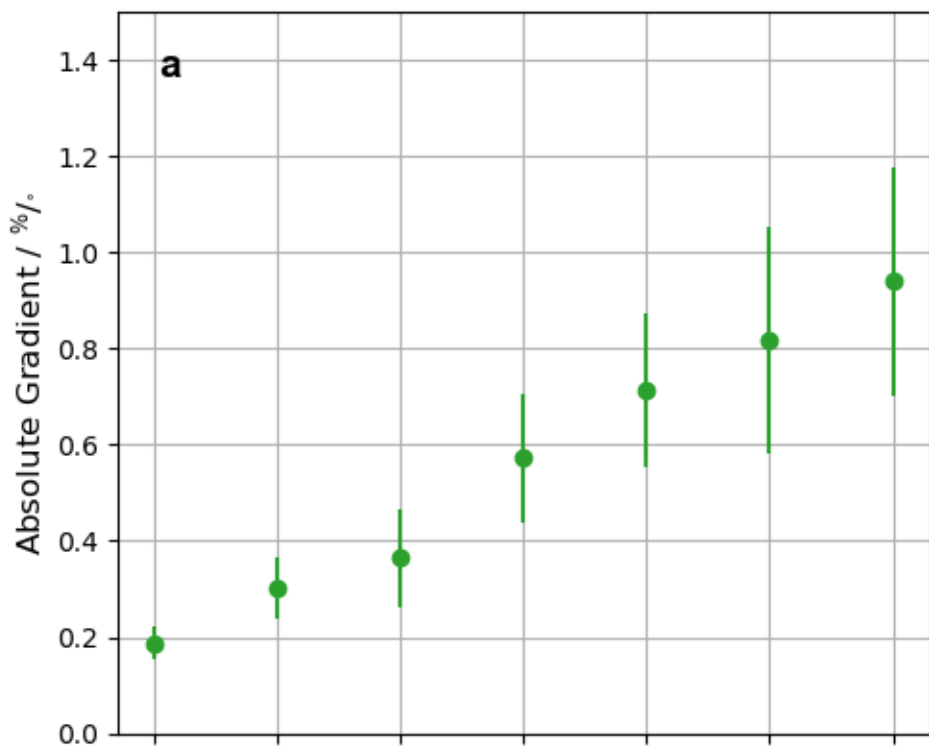
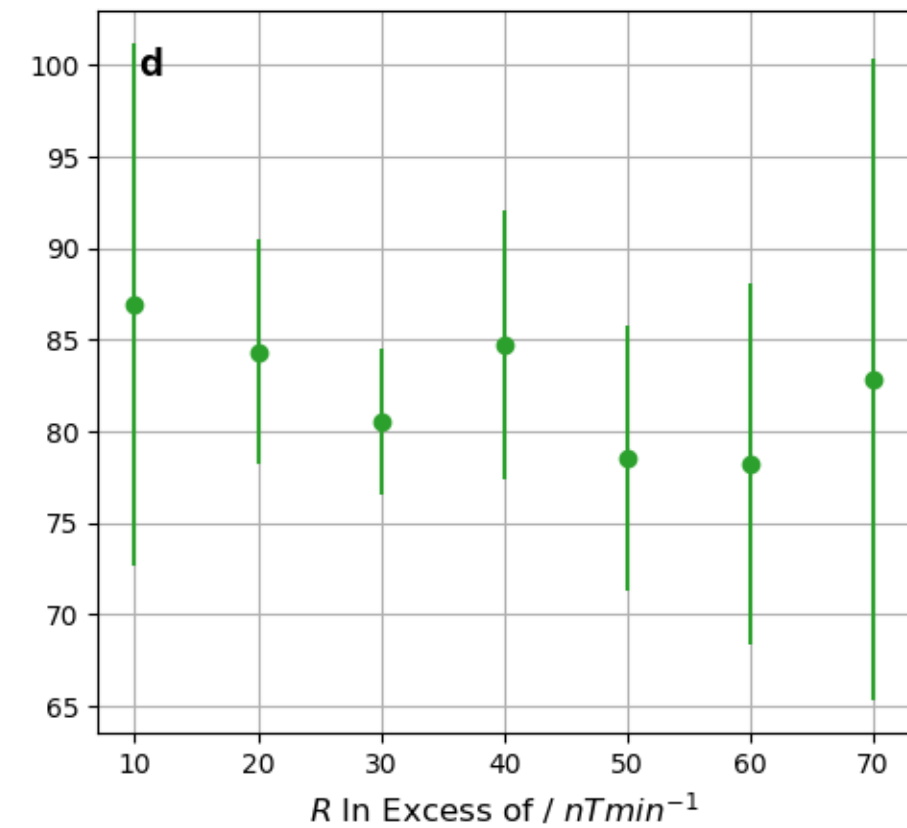
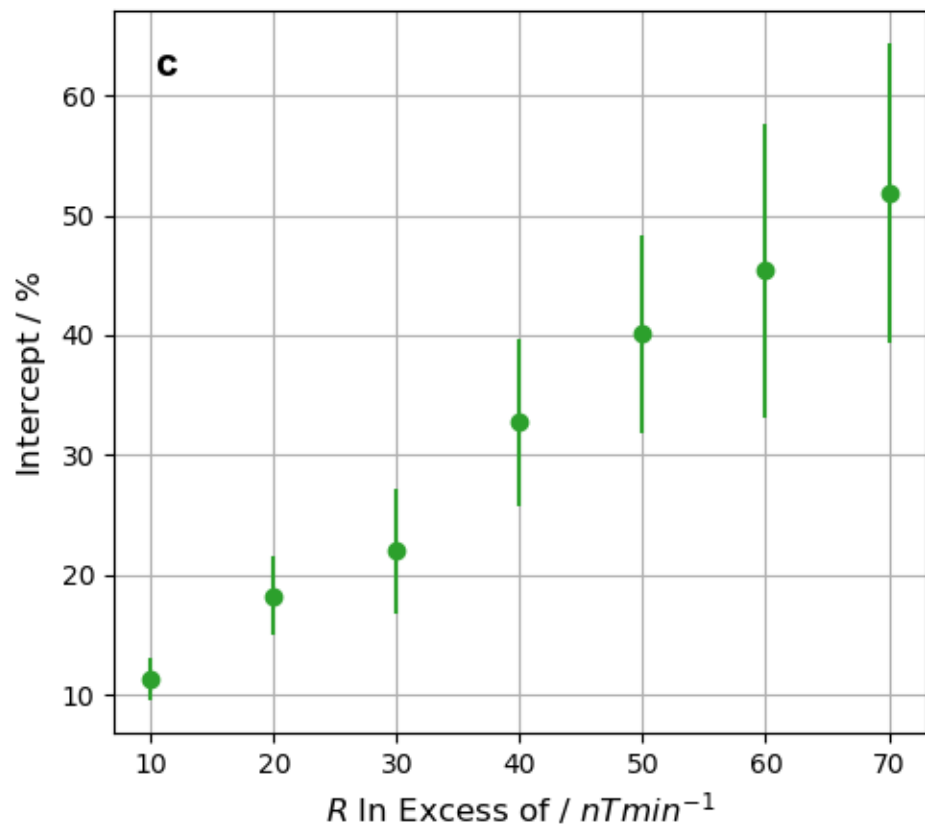
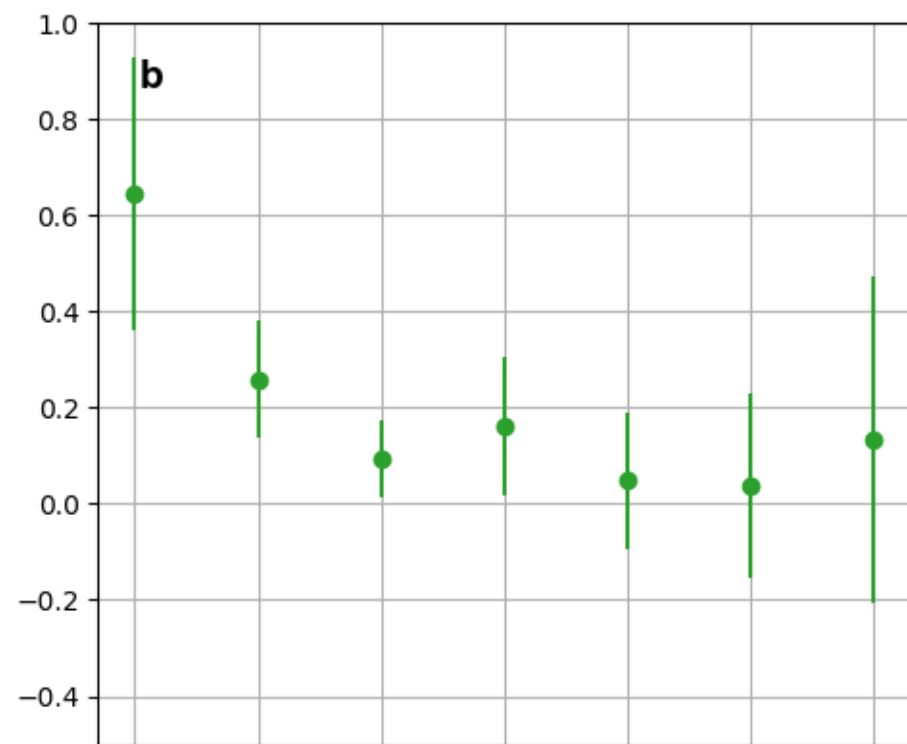
During SCs**SC + 1 Day**

Figure 7.

